JOURNAL OF GEOPHYSICAL RESEARCH, VOL. 99, NO. C3, PAGES 5095–5117, MARCH 15, 1994

Wind-forced variations in the Brazil-Malvinas confluence region as simulated in a coarse resolution numerical model of the South Atlantic

Linda T. Smith, Eric P. Chassignet, and Donald B. Olson

Rosenstiel School of Marine and Atmospheric Science, University of Miami, Miami, Florida

Abstract. The observed seasonal and interannual fluctuations in the Brazil-Malvinas confluence region are investigated using a wind-driven isopycnic coordinate model of the South Atlantic Ocean south of 10°S. The model is configured on a rotated Mercator grid with 2° horizontal resolution and five constant-density layers in the vertical. In order to model the passage of the Antarctic Circumpolar Current (ACC) across the basin, the grid is augmented by a channel extension to the west of Drake Passage and east of 50°E, having the width of Drake Passage. A series of benchmark experiments with annual mean climatological forcing shows that (1) when bottom topography is included, one observes a reduction in Drake Passage transport in agreement with previous studies, as well as a northward shift in the Brazil Current separation latitude, (2) an increase in Drake Passage transport to realistic values does not cause any further northward shift in the separation point, and (3) the model is relatively insensitive to the choice of lateral boundary conditions. A second set of experiments, in which the forcing is by seasonal climatological wind data and the Drake Passage transport is relaxed to a constant annual mean value, indicates the presence of a semiannual signal in the annual transport cycles for the Malvinas Current and for the ACC through Drake Passage. That signal is significantly damped in the Brazil Current region, and the amplitude of each cycle is reduced in comparison to observations. When the value to which the Drake Passage transport is relaxed is allowed to vary in time, the semiannual wind-forced oscillation in the Malvinas region remains evident, with additional superimposed variations related to the variations in the transport forcing. The final experiments are forced by a 10-year data set of realistic wind stress values, providing 10-year time series of model output for analysis of the interrelationships of the principal Southwestern Atlantic currents. A high correlation at the semiannual period is found to exist among the cycles of Drake Passage transport, Malvinas Current transport, and seasonal movements of the Brazil-Malvinas confluence latitude, while the Brazil Current transport cycle exhibits a significant energy peak only at the annual period. We conclude that the locally wind-forced semiannual signal south of the confluence is significantly damped before reaching the Brazil Current region by several factors: friction, the opposing flow of the current itself, and the inability of the Malvinas to penetrate the subtropical circulation that is confined to the upper model layers.

1. Introduction

The historical bias toward study of the northern half of the Atlantic Ocean has existed not only due to its inherently interesting physical characteristics but also as a consequence both of politics and of geography. Only recently has the South Atlantic been separately recognized for the features that distinguish it from the remainder of the world's oceans. The most scrutinized of these features to date has been the passage of the Antarctic Circumpolar Current (ACC) across the southern boundary of the ocean, from its entry through the bottleneck of Drake Passage to its broad outflow south of Africa. Present-day interest in the global-scale thermohaline circulation has focused attention on the seemingly anomalous equatorward transport of heat at middle and low latitudes in the South Atlantic, balanced by the deep southward flow of cold water which continues from the northern hemisphere [*Stommel*, 1980; *Roemmich*, 1983]. The interocean exchange that occurs when the Agulhas Current retroflection transports warm, saline Indian Ocean waters into the South Atlantic is also believed to play a role in the global balance of heat and salt [*Gordon*, 1986]. Recent studies of the Brazil Current have sought to quantify and explain its apparent differences in structure and transport from the western boundary current systems of other oceans, principally the Gulf Stream system in

Paper number 93JC03331.
0148-0227/94/93JC-03331$05.00

the North Atlantic, and to examine its separation from the coast and its confluence with the northward flowing Malvinas (Falkland) Current [*Zemba*, 1991; *Matano*, 1993; *Matano et al.*, 1993].

The Brazil-Malvinas confluence region extends eastward across the South Atlantic from the western boundary separation points of the two currents, one warm and saline, the other cold and relatively fresh. The confluence is typically characterized by a band of intermediate temperature surface waters, up to 300 km wide and filled with eddies, lying between the strong thermal fronts associated with each current [*Olson et al.*, 1988; *Gordon*, 1989]. The observed seasonal variability of excursions of the two currents along the coast suggests a signal that is predominantly annual for the Brazil Current and semiannual for the Malvinas, but with considerable interannual variation [*Olson et al.*, 1988]. Considering the relevant analytical study of *Anderson and Gill* [1975] and the North Atlantic basin scale model of *Anderson et al.* [1979], we expect the response of the western boundary currents in the South Atlantic to seasonal forcing to consist of a fast barotropic component over the relatively flat Argentine Basin, a longer-term response over topography tied to the interior baroclinic modes, and edge mode components from the ACC through the Subantarctic Front into the Malvinas proper.

The Malvinas originates in the northernmost of the system of fronts that characterize the ACC in Drake Passage, where the signal of eastward ACC transport has been shown to have both annual and semiannual components [*Peterson*, 1988; *Large and Van Loon*, 1989]. *Olson et al.* [1988] surmise that this seasonality may extend to the magnitude of northward Malvinas transport, to the location of the separation latitudes of the Brazil and Malvinas currents, and to the position of the confluence region across the basin. The existence of a seasonal cycle in Brazil Current transport may be related to seasonal fluctuations in wind stress over the gyre and/or to fluctuations in the northward Malvinas transport, either of which can lead to adjustment along the entire western boundary through edge wave propagation. Given that the Brazil Current transport is anomalously low compared to expectations based on integration of the wind stress over the subtropical gyre [*Veronis*, 1973], seasonal transport variations of the order of those found in the North Atlantic would, if present, constitute a significant percentage of the annual mean transport of the Brazil Current [*Olson et al.*, 1988].

Numerical modeling has, for the most part, represented the South Atlantic only as one element of the world ocean, in comprehensive studies that present a broad analysis of the major features of each basin (see, for example, *Bryan and Cox* [1972], *Cox* [1975], and *Semtner and Chervin* [1988, 1992]). Recent exceptions include the Fine Resolution Antarctic Model (FRAM) eddy-resolving calculation [*Webb et al.*, 1991], which covers the ACC passage through three ocean basins including the South Atlantic, and the work of *Matano* [1993], who models the South Atlantic from 20°S to 70°S with horizontal resolution varying from 1/2° to 1°, focusing on the mechanisms responsible for separation of the Brazil Current from the coast. Seasonal variations in climatological wind forcing are considered by *Matano et al.* [1993] in a study relating meridional movements of the confluence latitude to seasonal changes in the transport of the Brazil and Malvinas currents.

The numerical modeling effort reported herein seeks to investigate the observed seasonal and interannual fluctuations in the Brazil-Malvinas confluence region, specifically the variations in transport and configuration of the frontal zones associated with each current. Results are to be compared with recent direct and remote observations of the southwestern Atlantic [*Garzoli and Garraffo*, 1989; *Garzoli et al.*, 1992; *Provost et al.*, 1992; *Garzoli and Giulivi*, 1993] and with the numerical simulations mentioned above. A detailed numerical study of the processes involved in such issues, resolving the scales on which they occur, will call in the future for a fine-resolution model incorporating both wind and thermohaline forcing. However, much can be learned as a first step from the results of several coarse-resolution wind-driven experiments similar to those carried out by *Smith et al.* [1990] for the North and Equatorial Atlantic. Their model employs density as the vertical coordinate, allows the outcropping of constant-density layers, and is capable of handling relatively steep bottom topography [*Bleck and Smith*, 1990; *Smith*, 1992]. Adaptation of this model to the South Atlantic was straightforward, requiring only that satisfactory boundary conditions related to the inflow and outflow of the ACC be devised and tested.

In a series of benchmark simulations with annual mean climatological forcing, we find that (1) when bottom topography is included, we observe a reduction in Drake Passage transport in agreement with previous studies, as well as a northward shift in the Brazil Current separation latitude, (2) an increase in Drake Passage transport to realistic values does not cause any further shift in the separation, and (3) the model is relatively insensitive to the choice of lateral boundary conditions. When seasonal climatological wind forcing is included and the Drake Passage transport is relaxed to a constant annual mean value, we find the presence of a semiannual signal in the annual cycles of transport through Drake Passage and Malvinas Current transport, a significantly damped semiannual oscillation in the cycle of Brazil Current transport, and reduced amplitude in each cycle relative to observations. When the value to which the Drake Passage transport is relaxed is allowed to vary in time, the semiannual wind-forced oscillation in the Malvinas region remains evident, with additional superimposed variations related to the variations in the transport forcing. Turning from climatology

to the 1980-1989 European Center for Medium-range Weather Forecasting (ECMWF) wind data set, we construct 10-year time series of model output that allow analysis of the interrelationships of the major Southwestern Atlantic currents. A high correlation at the semiannual period is found to exist among the cycle of transport through Drake Passage, the cycle of Malvinas Current transport, and the cycle of seasonal movements of the Brazil-Malvinas confluence latitude. In the case of the Brazil Current transport cycle, a significant energy peak is found only at the annual period.

The paper is organized as follows. In section 2, we briefly describe the numerical model, focusing on its configuration for the South Atlantic and on the boundary conditions that apply to the ACC. Section 3.1 presents the results of experiments forced by the annual mean *Hellerman and Rosenstein* [1983] climatological wind data, including comparison of model integrations with and without bottom topography, and with and without forcing of the ACC transport through Drake Passage to a constant value. We then discuss the model results with forcing by the mean monthly *Hellerman and Rosenstein* [1983] data, both without and with temporal variation in the magnitude of the forced transport through Drake Passage (sections 3.2 and 3.3, respectively). In section 4 we turn to a 10-year model integration forced by the 10-year ECMWF wind stress data set. The experiments are discussed in section 5, and we conclude in section 6 by looking toward a more complex numerical representation of the South Atlantic basin.

2. Numerical Model

2.1. Model Equations

The isopycnic coordinate model of *Bleck and Boudra* [1986] has formed the basis for a number of ocean circulation studies, including the North and Equatorial Atlantic calculation of *Smith et al.* [1990], upon which the present study is based. The model configuration used by Smith et al. incorporated both variable coastline geometry and realistic bottom topography in a coarse resolution calculation (2° horizontal, five layers in the vertical) which verified the model's ability to reproduce the major features of the wind-driven circulation for the chosen domain.

The numerical details of the model are set out in *Smith et al.* [1990] and in its companion paper, *Bleck and Smith* [1990]. Here we present only the fundamental model equations before describing the specific configuration used for the South Atlantic calculation.

Under adiabatic flow conditions, the layer-integrated x and y momentum equations for each layer of constant density are

$$\frac{\partial u}{\partial t}+\frac{\partial}{\partial x}\frac{\mathbf{v}^2}{2}-(\zeta+f)v=-\frac{\partial M}{\partial x}+\frac{1}{\Delta p}[g\Delta\tau_x+\nabla\cdot(\nu\Delta p\,\nabla u)] \quad (1)$$

$$\frac{\partial v}{\partial t}+\frac{\partial}{\partial y}\frac{\mathbf{v}^2}{2}+(\zeta+f)u=-\frac{\partial M}{\partial y}+\frac{1}{\Delta p}[g\Delta\tau_y+\nabla\cdot(\nu\Delta p\,\nabla v)] \quad (2)$$

where $\zeta = \partial v/\partial x - \partial u/\partial y$ is the relative vorticity, $M \equiv gz + p\alpha$ is the Bernoulli function or Montgomery potential, α is the constant specific volume of the layer, Δp is the pressure thickness of the layer, $\Delta\tau_x$ and $\Delta\tau_y$ are the surface and bottom drag-related stress differences in x and y direction between the top and bottom of the coordinate layer, and ν is an eddy viscosity coefficient.

The wind-induced stress is assumed to linearly decrease to zero in the upper 100 m of the water column. (Note that at any given grid point, more than one layer of constant density may lie within that 100 m depth.) In the flat bottom experiment to be described in section 3.1.1, bottom friction is incorporated by assuming a linear stress profile in a boundary layer of 10 m thickness using a standard bulk formula with drag coefficient 0.003. Bottom drag is not included in the remaining experiments.

The eddy viscosity ν is one that reverts from a value $u_d\Delta x$ to a value proportional to the total deformation, $[(u_x - v_y)^2 + (v_x + u_y)^2]^{1/2}\Delta x^2$, in regions of large horizontal shear [*Smagorinsky*, 1963]. Here Δx is the horizontal grid size, u_d is a background diffusive velocity, and subscripts denote partial derivatives. Note that expressing the lateral viscosity coefficient as the product $u_d\Delta x$ (units of squared meters per second) and holding u_d constant corrects ν for variations in grid resolution within the model domain.

The third equation solved in each constant-density layer is the nonlinear continuity equation. Under adiabatic conditions, the equation is

$$\frac{\partial}{\partial t}(\Delta p)+\frac{\partial}{\partial x}(u\Delta p)+\frac{\partial}{\partial y}(v\Delta p)=0. \quad (3)$$

The continuity equation is solved by the Flux-Corrected Transport method [*Zalesak*, 1979], which permits the existence of massless grid points ($\Delta p = 0$) at any location in the model domain while maintaining the nonnegative character of the layer thickness field.

2.2. Model Configuration

In the north-south direction, the model domain includes the South Atlantic Ocean from 10°S to the Antarctic continent, the southernmost coastal point of which lies near 80°S in that sector. The equatorial Mercator projection used by *Smith et al.* [1990], in which the northernmost point considered is 62°N, would in the present case require a horizontal grid size at high latitudes that is roughly one sixth of that near the equator. Since this distortion would severely limit the maximum permissible time step for the numerical calculation, we choose instead a rotated Mercator projection whose "equator" coincides with the true 10°W meridian. (The "north pole" in this projection would then

lie on the true equator at 100°W.) The model's horizontal resolution is a constant 2° of true latitude along the meridian 10°W. Perpendicular to 10°W, the mesh size decreases with the cosine of "latitude" in both directions away from 10°W (the "equator"), so that grid boxes remain square. In this projection, shown in Figure 1, there are 39 grid points in the direction parallel to 10°W and 40 points in the direction perpendicular to that meridian.

North of Drake Passage, the east coast of South America forms the western boundary for the model ocean. On the eastern side, the domain is bounded by the African coast, and then by an artificial wall which extends south from the southern tip of Africa to 45°S and thence diagonally to the southeastern corner of the grid (Figure 1). The placement of this wall precludes any exchange of water between the Indian and South Atlantic oceans in the model region south of Africa, such as might exist in an eddy-resolving calculation that would allow rings from the Agulhas retroflection to form and propagate westward. For the purpose of modeling the passage of the ACC across the South Atlantic, the grid is augmented by a channel extension lying to the west of 70°W (Drake Passage) and to the east of 50°E, having roughly the width of Drake Passage. The outer walls of this channel extension are drawn parallel to the central meridian (10°W), while the inner channel boundaries coincide with the Antarctic coastline. The extension is terminated approximately 20° of longitude to the west of Drake Passage, and equivalently on the eastern side of the basin, so that the length of the modeled ACC channel is 160° of longitude along 60°S.

Also shown in Figure 1 is the bottom topography used in the majority of our model experiments. The topography was derived on the 2° rotated Mercator grid from the 1/12° ETOPO5 data set obtained from the National Geophysical Data Center, Boulder, Colorado. In order to retain the relatively abrupt changes of the bathymetry, the only smoothing applied to the data was done by hand to remove "spikes" and single zero-depth points. To forestall wave breaking along shallow continental shelves, the bottom depth is set to 200 m from the coastline to the 200 m isobath.

In the vertical, the model is configured with five layers

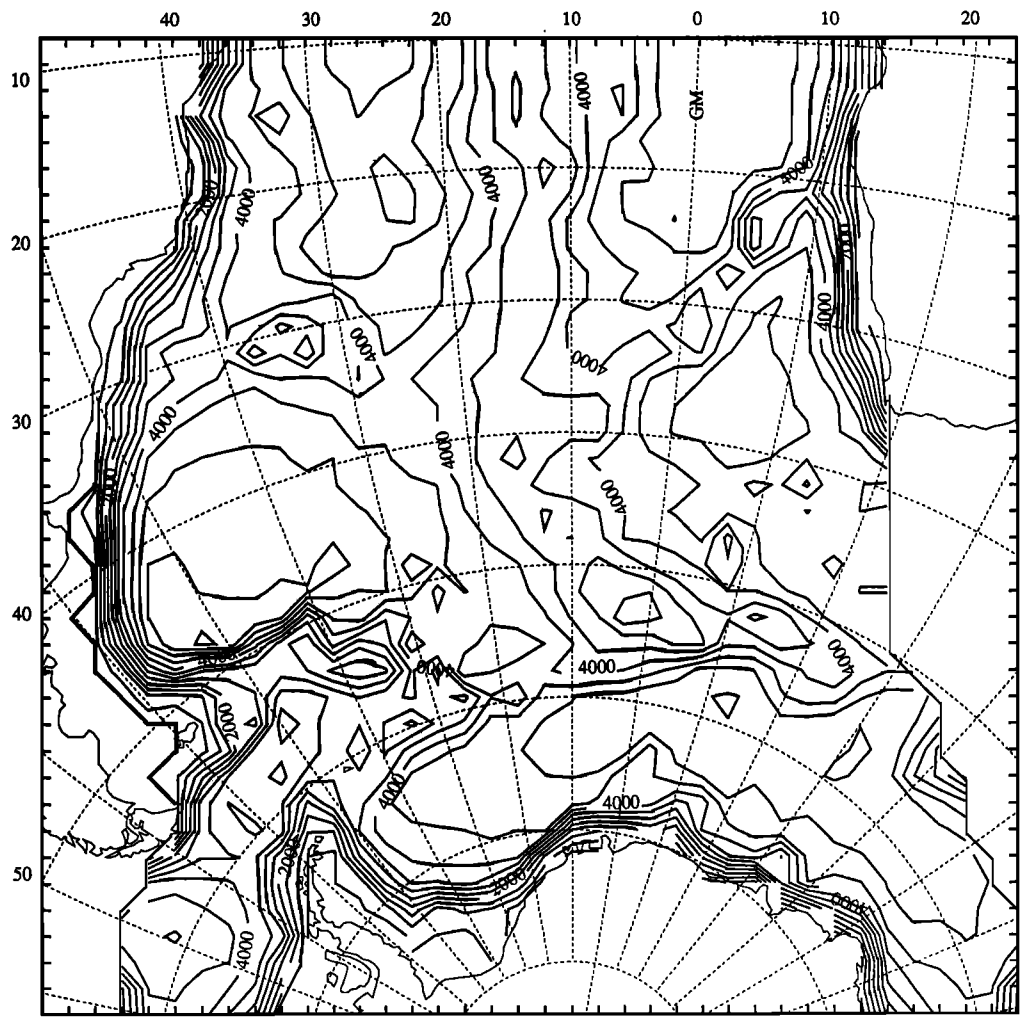

Figure 1. Model basin and bathymetry. Contour interval is 500 m. Depths on the continental shelf (inshore of heavy line) are set to 200 m.

of constant density. The initial mass distribution (Figure 2) is patterned after the annual mean zonal average density distribution for the South Atlantic presented by *Levitus* [1982]. Spin-up of the model is accomplished in the first year of integration due to the rapid geostrophic adjustment that results from imposition of the density structure on a motionless ocean. The density values assigned to the five isopycnal layers, also taken from *Levitus* [1982], are (in σ units) 25.4, 26.5, 27.0, 27.5, and 27.9. Note that bottom topography may truncate the layer structure shown in Figure 2.

All model experiments were carried out with no-slip lateral boundary conditions along coastlines and artificial walls of the basin, with the exception of one sensitivity study (described in section 3.1.3) in which free-slip boundary conditions were used. Cyclic lateral boundary conditions are imposed between the westernmost and easternmost edges of the ACC channel extension described above, effectively creating a continuous pathway around Antarctica. Although the use of open boundaries, together with "sponge layers" designed to minimize wave reflection at those boundaries, may be considered a more physically realistic method of modeling the ACC passage across the basin, solving the primitive equations in the presence of such boundaries is not a well-posed problem [*Oliger and Sundström*, 1978]. The cyclic conditions employed herein have the advantages of numerical stability and simplicity, while easily allowing the incorporation of methods designed to force the ACC transport through Drake Passage toward realistic values. The numerical implementation of the cyclic boundary conditions is described in the Appendix.

The experiments to be described below are summarized in Table 1, which notes the case-by-case differences in forcing, bathymetry, boundary conditions, and lateral and bottom friction.

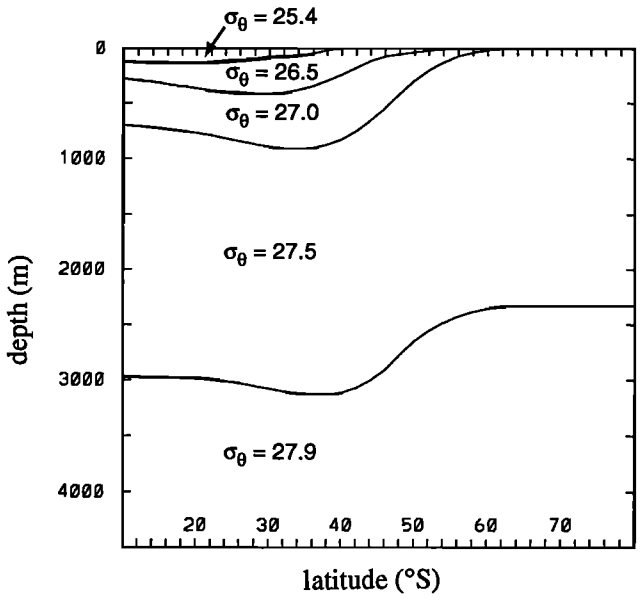

Figure 2. Meridional cross section showing initial mass field. Solid lines are layer interfaces.

3. Model Experiments Forced by Climatological Wind Data

3.1. Model Experiments Forced by Annual Mean Winds

In Figure 3a we show the stress vectors for the annual mean winds of *Hellerman and Rosenstein* [1983] (hereafter HR83), interpolated onto the rotated Mercator grid of Figure 1. Four model experiments forced by these winds were carried out in order to test the model's sensitivity to (1) bottom topography, (2) imposed forcing of the ACC velocities at Drake Passage, and (3) lateral boundary conditions. In each case the model was initialized with the mass distribution described in the preceding section.

3.1.1. Flat bottom versus rough bottom. We refer to our first two experiments as FB (Flat Bottom) and RB (Rough Bottom), differing only by the inclusion of the topography of Figure 1 in the latter. Both case FB and case RB reached a steady state using a value of 20 cm s^{-1} for the diffusive velocity u_d (giving an eddy viscosity coefficient of 3.5×10^4 m^2 s^{-1} at midbasin). Bottom drag was included for case FB only, as a standard bulk formula with drag coefficient 0.003. In both experiments, no-slip lateral boundary conditions were imposed along coastlines and artificial walls of the basin.

Contours of the barotropic (depth-integrated) streamfunction are shown in Figure 4a for case FB and in Figure 4b for case RB. The most conspicuous difference between the results of these two cases lies in the transport of the ACC across the model basin. Measured at Drake Passage, 309 Sv (1 Sv $\equiv 10^6$ m^3 s^{-1}) are obtained in the flat bottom case, as opposed to 67 Sv in the case with topography. This difference in transport may be compared qualitatively to that found in the results of *Bryan and Cox* [1972] and *Cox* [1975] for a 2° model of the world ocean. For a barotropic case with constant bottom depth 5000 m and lateral friction roughly equivalent to that of case FB, *Bryan and Cox* [1972] obtained 600 Sv through Drake Passage at the end of 90 days of integration. *Cox* [1975] found that adding bottom topography to the same model (but with lateral friction twice as large) reduced the transport to only 22 Sv. Numerical simulations by *McWilliams et al.* [1978], *Treguier and McWilliams* [1990], and *Wolff et al.* [1991] have demonstrated the importance of topographic drag as the principal sink for momentum in the ACC. Inclusion of bottom topography was found in their experiments to reduce the model ACC transport by an order of magnitude in comparison to its value in flat bottom calculations, where bottom friction and lateral eddy viscosity were the only means for removing energy from the system.

When baroclinicity was included in the *Cox* [1975] world model with bottom topography, in an experi-

Table 1. Summary of Model Experiments

Case	Bathymetry	Wind Forcing	Lateral Boundary Condition	u_d, cm s^{-1}	Bottom Drag Coefficient	ACC Transport Forcing
FB	flat	mean HR	no-slip	20	0.003	no
RB	rough	mean HR	no-slip	20	0.	no
RBL	rough	mean HR	no-slip	5	0.	no
RBF	rough	mean HR	no-slip	5	0.	yes
RBFS	rough	mean HR	slip	5	0.	yes
RBFM	rough	monthly HR	no-slip	5	0.	yes
RBFE	rough	mean ECMWF	no-slip	5	0.	yes
RBFME	rough	monthly ECMWF	no-slip	5	0.	yes

FB is flat bottom; RB is rough bottom; RBL is rough bottom, low viscosity; RBF is rough bottom, forced; RBFS is rough bottom, forced, slip boundary condition; RBFM is rough bottom, forced, monthly winds; RBFE is rough bottom, forced, ECMWF winds; RBFME is rough bottom, forced, monthly ECMWF winds.

ment with nine levels in the vertical and temperature and salinity as prognostic variables, the model ACC transport increased to 184 Sv, versus the 22 Sv of his barotropic rough bottom case. Approximately the same value, 180 Sv, is obtained in the global eddy-resolving calculation of *Semtner and Chervin* [1988, 1992], while the FRAM model of the Southern Ocean [*Webb et al.*, 1991] produces 195 Sv through Drake Passage after only 6 years of integration. The ACC transport magnitude obtained in these previous studies is roughly 1.5 times the observed figure of approximately 130 Sv reported by *Whitworth et al.* [1982] and *Peterson* [1988]. *Garzoli et al.* [1992], in comparing the temperature fields of the *Semtner and Chervin* [1992] model to sea surface temperature (SST) data from satellite observations, note that the model ACC transport may be higher than observed due to insufficient resolution of the sharply sloping topography in the Drake Passage–Malvinas Plateau region. A similar remark concerning the resolution of topography is made by *Webb et al.* [1991]. In comparing our results to other modeling studies, it must be kept in mind that our ACC channel is wind forced on only 160° and that thermodynamics are not included. These factors, as well as differences in horizontal and/or vertical resolution, are likely to contribute significantly to the difference in calculated transport magnitudes.

The model subtropical gyre circulation is confined primarily to the upper two layers in case RB but extends to the fourth layer in the FB results due to the absence of topography and consequent greater depth of the fluid. In both cases, the uppermost layer outcrops poleward of the subtropical region. Separation of the western boundary current from the coast can be defined by the locus of that outcropping line, as in the model of *Parsons* [1969]. In the layer 1 velocity vectors for the FB and RB results (Figures 4a and 4b), it can be seen that the inclusion of bottom topography in case RB has the effect of shifting the separation latitude of the Brazil Current to a realistic 38°S [*Olson et al.*, 1988], approximately 5° north of its position in case FB. The topography of case RB allows the Malvinas Current to ride northward along the continental

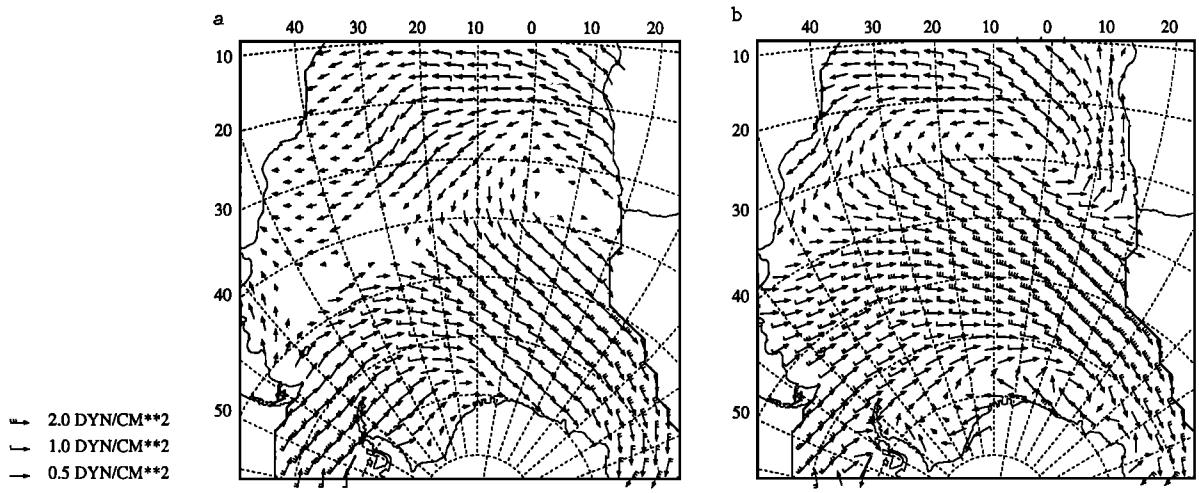

Figure 3. (a) Annual mean *Hellerman and Rosenstein* [1983] wind stress vectors over the model domain. (b) Mean wind stress vectors for the 1980-1989 ECMWF data set over the model domain.

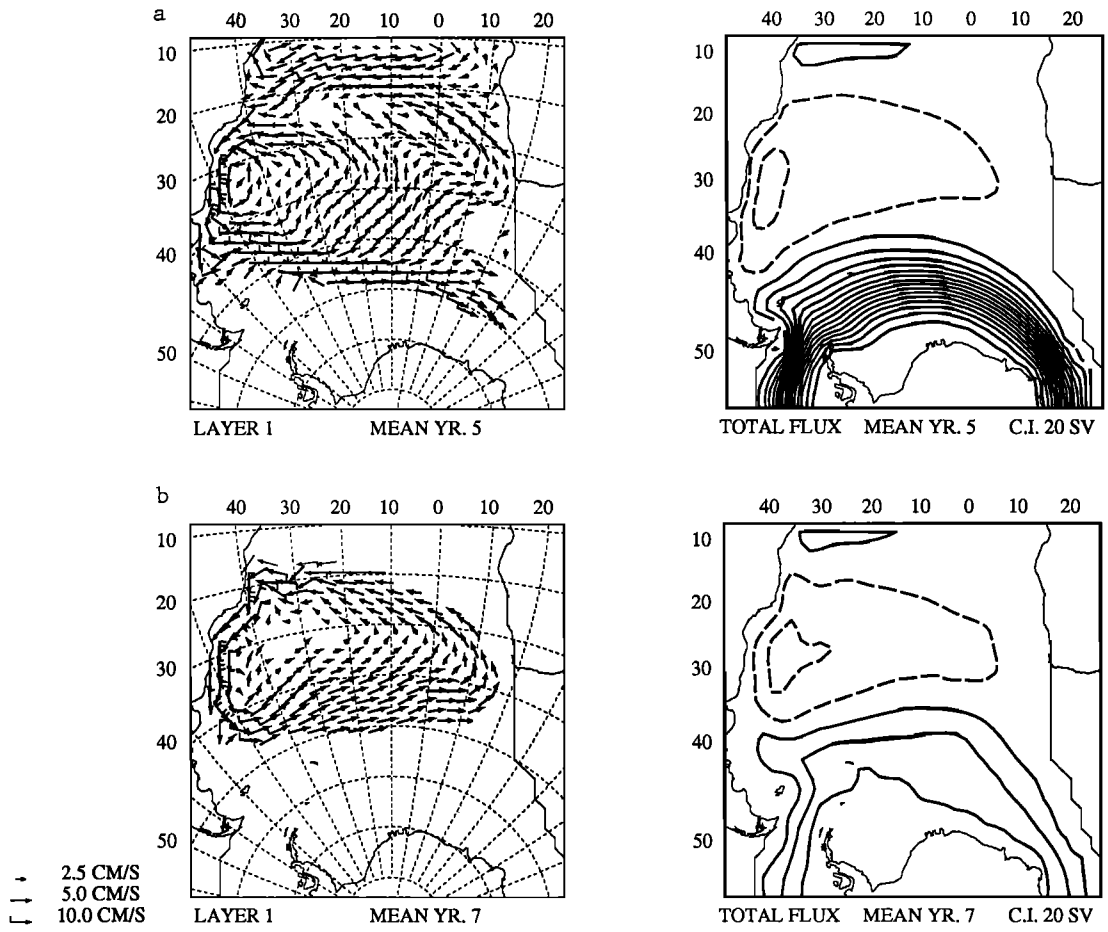

Figure 4. Layer 1 velocity vectors and barotropic mass flux streamfunction: (a) experiment FB (flat bottom, nonforced) and (b) experiment RB (rough bottom, nonforced). (Diffusive velocity $u_d = 20$ cm s^{-1}.) C.I. $\equiv$ contour interval. Solid (dashed) lines denote cyclonic (anticyclonic) flow. The zero contour is not drawn.

slope to $\sim 40°$S before turning to the interior, in contrast to the eastward turn along 48°S in the flat bottom case. *Matano* [1993] notes the importance of topography in determining the path both of the ACC and of the Malvinas, which branches from it. Because of its predominantly barotropic character, the ACC will tend to flow along contours of planetary potential vorticity f/H, which can be traced from Drake Passage to the continental slope off Argentina.

3.1.2. Drake Passage velocities forced versus nonforced. Our second set of model experiments focuses on the effect of forcing the ACC transport through Drake Passage toward a realistic value. We compare the above rough bottom experiment to experiment RBF (Rough Bottom, Forced), in which a forcing term is included in the along-channel barotropic momentum equation for those grid points that lie along the end of the ACC channel extension to the west of Drake Passage. The added forcing term is a Newtonian relaxation of the form $\mu(v^{(0)} - \bar{v})$, where the relaxation coefficient μ has units of inverse time, $\bar{v}$ is the barotropic velocity of the model, and $v^{(0)}$ is the barotropic velocity toward which $\bar{v}$ is to be driven.

The velocities $v^{(0)}$ for each grid point are determined with the intention of increasing the model transport through Drake Passage to observed values. On the basis of both relative geostrophic shear from hydrographic surveys and direct current measurements, *Whitworth et al.* [1982] estimate the average transport through the passage to be 130 Sv. Our method for determining the values of $v^{(0)}$ is as follows. First, the geostrophic velocities across Drake Passage, at each grid point and in each layer, are calculated from the *Levitus* [1982] data set for the mass distribution used to initialize the model integration. Second, the transport through the Drake Passage section which results from these velocities is determined. Third, we calculate the single barotropic velocity which, when added at each grid point of the section, increases the transport to a value of 130 Sv. Finally, the transport through each grid column, that is, the sum of the geostrophic and added barotropic velocities for each layer times the thickness of the layer times the grid column width, is calculated. Dividing that transport by the depth of the grid column times its width gives the velocities $v^{(0)}$ required to achieve a transport of 130 Sv. *Matano* [1993] arrives at a similar result by imposing the value of the streamfunction (120

Sv in his benchmark experiment) on the open western boundary that represents Drake Passage in his model.

The values of $\mu = (1 \text{ hour})^{-1}$ and $u_d = 5$ cm s^{-1} were retained for the final 5 years of integration of experiment RBF. This value of u_d gives a relatively low lateral eddy viscosity coefficient, needed for a numerically stable solution. The fast relaxation time of 1 hour strongly forces the transport through Drake Passage to 128 Sv, allowing for essentially no variation in time from that value throughout the model run with constant wind forcing. In section 3.3, we will discuss the results of experiments in which the relaxation time is equally fast but the value to which the transport is forced is allowed to vary from day to day. Experiments carried out with longer relaxation times failed to bring the Drake Passage transport value near to the desired value of 130 Sv.

For direct comparison to case RBF, the nonforced rough bottom experiment RB described in the preceding section was integrated for an additional 2 years with $u_d = 5$ cm s^{-1}. We refer to this as experiment RBL (Rough Bottom, Low viscosity). The previous value of 20 cm s^{-1} used in RB was needed only for comparison to the flat bottom case FB, which required the higher value of lateral eddy viscosity due to the absence of any topographic sink for energy.

The layer 1 velocity vectors and contours of the barotropic streamfunction for case RBF ($u_d = 5$ cm s^{-1}) are shown in Figure 5. The model results have been averaged over the final year of integration for display. The impact of the forcing of velocities through Drake Passage is evident in the RBF results, with the transport through that section increased to 128 Sv from the 69 Sv obtained in the nonforced case RBL (similar to case RB, Figure 4b). The forced case also shows the Malvinas Current transport reaching 68 Sv within a recirculation centered on ~ 45°S, versus only 22 Sv at that latitude in the RBL results. Although few observations are available from the Malvinas region, a significant barotropic component is believed to exist in the current. *Peterson* [1992], on the basis of a hydrographic survey, estimates the depth-integrated transport to be as high as 75 Sv at 42°S. This may be a reasonable consequence of the northward movement of water from Drake Passage over the Falkland Plateau, overriding the deep current which is also flowing to the north.

In the subtropical gyre region, the RBL and RBF solutions are very similar. In both cases, the model Brazil Current separates from the coast at ~ 38°S, and the barotropic transport of the gyre reaches 35 Sv within the western boundary recirculation region at 30°-35°S. Of the total transport, nearly 30 Sv is carried in the uppermost three model layers, which taken together extend to ~ 1000 m at the deepest part of the gyre. A comparison of these results to observations is limited due to the wide variations that exist in published values of observed Brazil Current transport, depending both on latitude and on the chosen reference depth. Additionally, our numerical solution does not include the thermohaline-driven North Atlantic Deep Water (NADW), and therefore the model results in this regard represent only the wind-driven component of the gyre transport. *Gordon and Greengrove* [1986] report that the Brazil Current attains transport values of 19-22 Sv at 38°S (relative to 1400 m), owing to a recirculation cell south of 30°S. North of that latitude, transport values are reported as low as 4 Sv between 10° and 20°S, where the current is shallow and closely confined to the continental shelf [*Stramma et al.*, 1990]. South of ~ 38°S, as the current turns offshore and rides over the southward flowing NADW, total transport relative to 3000 m has been estimated at 76 Sv by *Zemba* [1991].

The model solution in the confluence region of the Brazil and Malvinas currents is illustrated by means of the layer 2 and 3 velocity vectors for cases RBL (Figure 6a) and RBF (Figure 6b). In the RBF (forced) case, an intensified northward flow is noticeable along the coast northwest of Drake Passage in both layers, but the eastward turning point of the two currents after separation from the coast, ~ 40°S, differs little from the RBL (nonforced) case. This is in contrast to the results of *Matano* [1993], who found that the point of separation shifted 5° to the north when the imposed model transport through

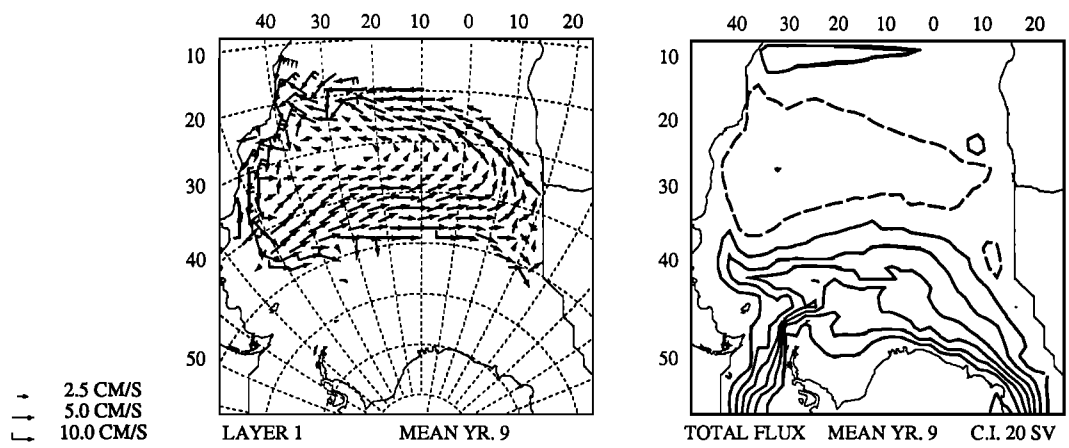

Figure 5. As in Figure 4 for experiment RBF (rough bottom, forced). ($u_d = 5$ cm s^{-1}.)

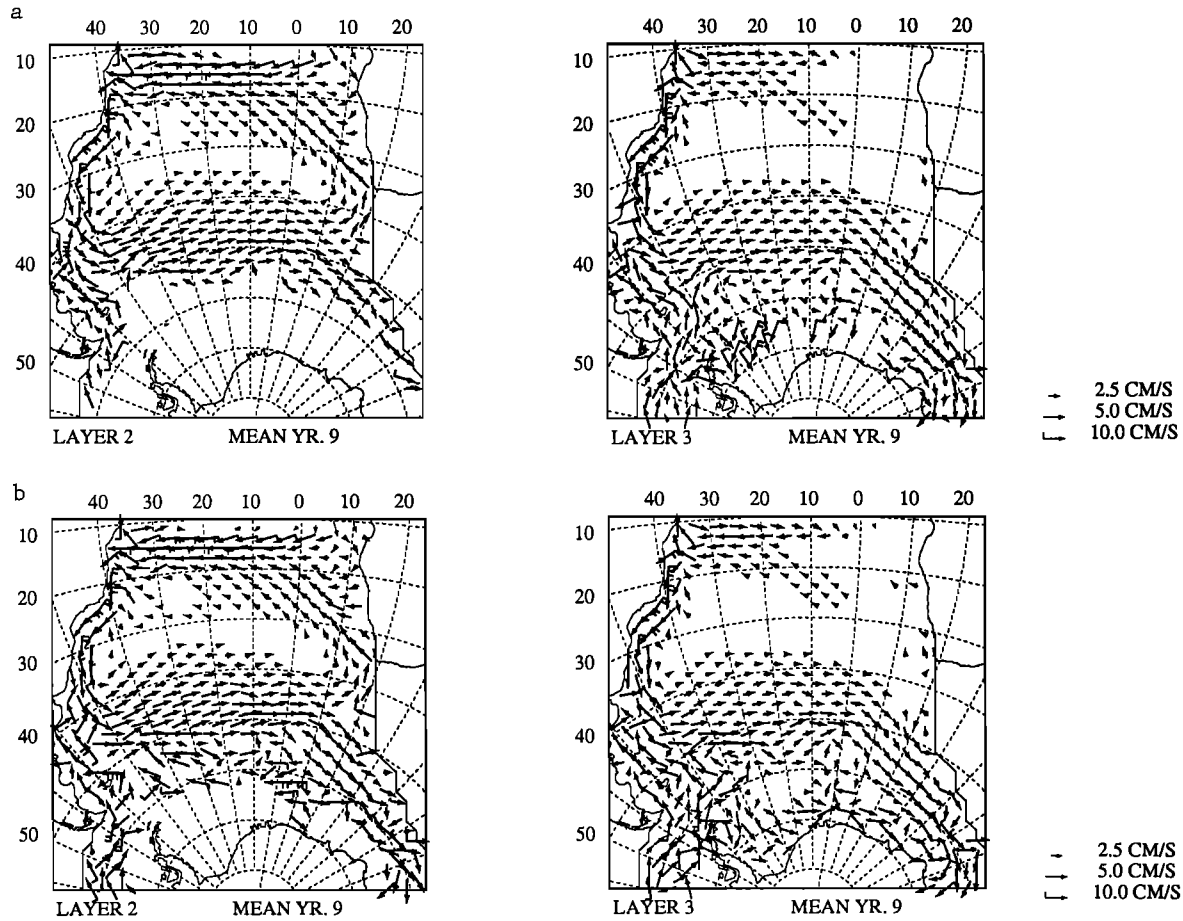

Figure 6. Layer 2 and 3 velocity vectors: (a) experiment RBL and (b) experiment RBF.

the open boundary at Drake Passage, and consequently the Malvinas transport, was increased to 180 Sv versus the inflow value of 120 Sv used in his initial experiment. In that initial case, separation of the currents from the coast occurred at ~ 45°S, the latitude of zero wind stress curl. In the present model, however, separation from the western boundary is related to the tilting and packing of isopycnal surfaces associated with the outcropping of constant-density layers, the configuration of which depends primarily on integral properties of the applied wind stress [*Parsons*, 1969; *Veronis*, 1973; *Huang*, 1986; *Chassignet and Bleck*, 1993]. In an additional experiment forced by constant winds and with the model ACC transport further increased to 180 Sv (not illustrated), the subsequent intensification in Malvinas Current transport, which brings about the northward relocation of the separation point in *Matano's* [1993] model, was again found to play no significant role in relocating that point in our simulations. The inclusion of bottom topography, however, is of great importance, as noted in the previous section.

The eastward turning point of the model Brazil and Malvinas currents, ~ 40°S (Figure 6b), is in reasonable agreement with satellite observations, which place the annual mean position of the confluence between 36°S and 39°S at the western edge of the basin [*Olson et al.*, 1988]. While the broad features of the confluence region are visible in the results of experiment RBF (Figures 5 and 6b), the fine structure of eddies and meanders that exists between the two currents is not resolved by our coarse-resolution experiments. On the eastern side of the model basin, Figures 5 and 6 show the subtropical convergence located ~ 5° south of its observed mean position of 40°S [*Peterson and Stramma*, 1991]. We attribute this to the tendency of the model ACC to bend southward as it flows along the artificial wall leading to the eastern channel extension and thence into Drake Passage.

3.1.3. No-slip lateral boundary conditions versus free-slip conditions. Model case RBFS (Rough Bottom, Forced, Slip) was integrated for 5 years beginning from the final year of case RBF, with slip boundary conditions imposed on all coastlines and artificial walls of the model basin, as opposed to the no-slip conditions used for RBF. All other parameters for RBFS are identical to those of RBF, and the model output (not illustrated) was averaged over the final year of integration.

Apart from small-scale features, principally along the eastern model boundary, the two solutions are very similar. In particular, transport through the Drake Passage

section is 130 Sv for case RBFS versus 128 Sv for RBF, and the Brazil Current separation latitude remains at ~ 38°S. The latter result is not surprising, since the separation is associated with the outcropping of the upper layer, a large-scale response which is dependent upon integral properties of the applied wind stress but in principle independent of the choice made for the lateral boundary condition [*Chassignet and Bleck*, 1993].

3.2. Model Experiments Forced by Seasonal Winds

Beginning from the solution for case RBF, the model was integrated for 10 years with forcing by the mean monthly wind stress data of HR83. All other parameters for this case, which we refer to as RBFM (Rough Bottom, Forced, Monthly winds), are identical to those of RBF.

The 10-year series of transport through Drake Passage from the RBFM results is shown in Figure 7a, and the corresponding series of Malvinas Current transport across 45°S in Figure 7b. Although the wind forcing is identical from year to year, the annual cycle of transport values produced by the model exhibits some variation in time due to the presence of nonlinear effects. We show the entire series, rather than an average over the 10 years, in order to facilitate comparison with the results of the next section, in which we discuss a model integration with forcing by the 10-year ECMWF wind data set.

A semiannual signal can be discerned in both the Drake Passage and Malvinas transport cycles (Figures 7a and 7b), with significantly smaller amplitude in the case of the former due to the strong relaxation of the transport to a constant value. Analyses of the coherence and phase relationship between each of these 10-year series and the zonally averaged wind stress curl of the HR83 monthly winds along 45°S (repeated 10 times) indicate a high correlation between transport and wind stress curl at the semiannual period. We therefore surmise that the seasonal variations in each cycle are a local response to the semiannual signal present in the zonally averaged wind stress curl over the region south of ~ 35°S [*Olson et al.*, 1988, Figure 8c]. This is in agreement with the results of *Garzoli and Giulivi* [1993] relating seasonal variability in the confluence region to local changes in the curl of the wind stress. Analysis of the phase relationship between the two annual transport cycles from the RBFM results (Figures 7a and 7b) additionally shows that the June maximum in Malvinas transport, occurring at the time of strongest winter winds, and the secondary maximum in December (summer), lag approximately three months behind the March and September maxima in transport through Drake Passage. In section 4.2, we will present a more complete discussion of similar coherence and phase analyses between pairs of 10-year time series from a model run forced by the ECMWF wind data set.

Contours of the barotropic streamfunction for the months of March and June, taken from an average annual cycle created from the 10-year RBFM run, are displayed in Figure 8. The slight difference between the two months in Drake Passage transport (less than 3 Sv) cannot be seen in the figures. However, the dividing line between the subtropical and subpolar gyres (i.e., the line of zero streamfunction value) clearly shifts to the north by ~ 4° along 45°W in the month of June, the month of strongest winter winds and maximum Malvinas transport. We define this dividing line to be the "confluence" of the Brazil and Malvinas currents in the model results. As with our previous definition of the line of western boundary current separation as the locus of the upper layer outcrop, this provides an unambiguous determination of the confluence location for the purpose of discussion. Analysis of the coherence and phase relationship between the 10-year series of the confluence latitude along 45°W from experiment RBFM and the zonally averaged wind stress curl of the HR83 winds along 45°S indicates, as in the case of Malvinas and Drake Passage transport, a high correlation between confluence location and wind stress curl at the semiannual period. The northward movement of the confluence latitude in early winter (June) is associated with the absolute maximum in negative wind stress curl along 45°S which occurs at that time of year, while the opposite holds true in March, i.e., a southward movement of the confluence in relation to a maximum in positive curl over the region. A similar result is found by *Matano et al.* [1993], who relate meridional movements of the con-

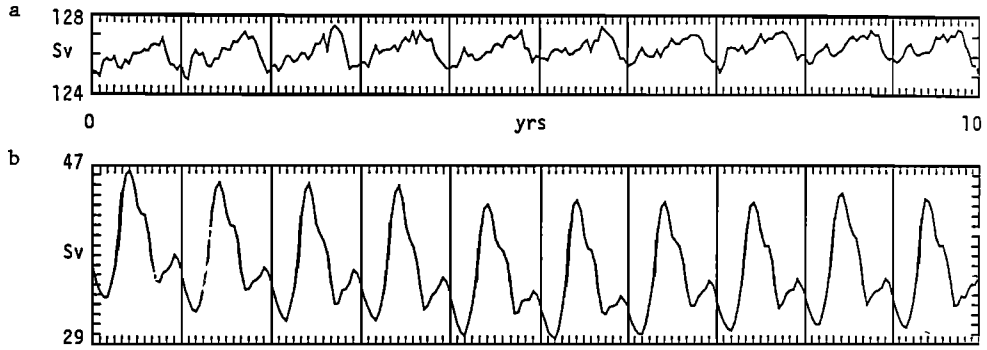

Figure 7. 10-year series of transport, experiment RBFM (rough bottom, forced, monthly winds): (a) Drake Passage and (b) Malvinas Current across 45°S.

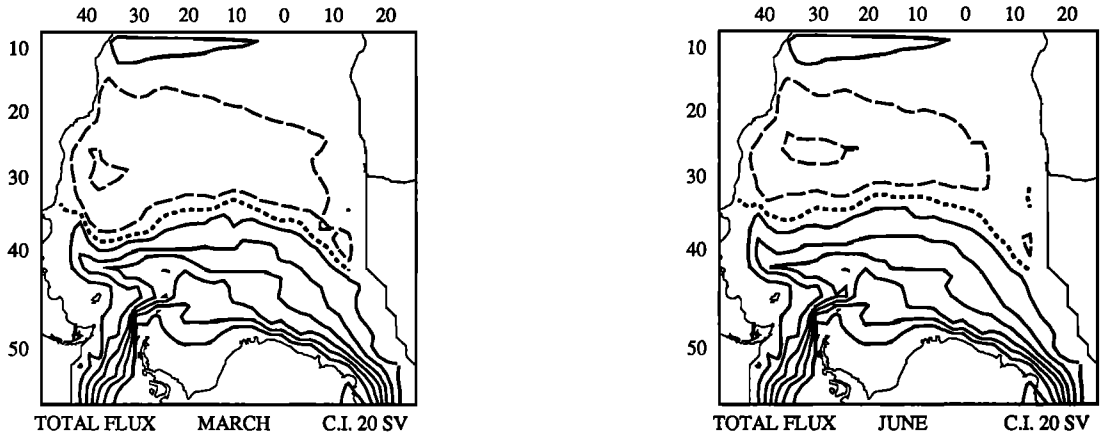

Figure 8. Barotropic mass flux streamfunction for the months of March and June from average annual cycle of experiment RBFM. Short-dashed line denotes zero contour.

fluence latitude to seasonal changes in the transport of the Brazil and Malvinas currents. Using a barotropic numerical model forced by the HR83 monthly winds for the subtropical gyre together with Geosat altimeter data for the Malvinas Current region, they find that the confluence latitude is displaced to the south in austral summer, when the subtropical gyre flow accelerates and the Brazil Current transport reaches a maximum. Conversely, an increase in the Malvinas transport in winter is accompanied by a northward movement of the confluence latitude.

The strong semiannual signal associated with the Malvinas transport can also be seen in the barotropic streamfunction anomaly (relative to the annual mean) from the average annual cycle of experiment RBFM. The anomaly for the months of March, June, September, and December is shown in Figure 9, partitioned into the transport for layers 1 and 2, and for layers 3, 4 and 5. In the lower three layers, the semiannual Malvinas signal is evident from $\sim$ 30°-50°S, as the anomaly alternates between positive and negative values. In the upper two layers, the anomaly of Brazil Current transport exhibits only a weak semiannual signal in the region between 30° and 40°S. Two factors may contribute to this significant damping of the semiannual oscillation. First, the predominant signal in the zonally averaged wind stress curl is annual to the north of $\sim$ 35°S [*Olson et al.*, 1988]. Second, the response to semiannual fluctuations in the wind stress curl south of that latitude, which can affect the magnitude of northward Malvinas transport, may in the case of the Brazil Current be blocked by the southward flow of the current itself.

Observations indicate that the seasonal cycle of eastward ACC transport through Drake Passage has both annual and semiannual components, with the amplitude of the highly variable annual cycle ranging up to 40 Sv and with relative maxima occurring each spring and fall [*Whitworth*, 1983; *Peterson*, 1988]. The seasonal cycle of Malvinas Current separation from the coast also is believed to possess a semiannual signal related to the Drake Passage seasonal variations. Observations place the point of separation further to the north in austral winter (July to September) than in summer (January to March), with an annual range of up to 850 km along the coast. Similar characteristics apply to the separation point of the Brazil Current, although evidence of a well-defined annual signal is lacking [*Olson et al.*, 1988].

Results of the model run RBFM agree with these observations in terms of phase, although the amplitude of the seasonal variations is greatly reduced. In the case of the Drake Passage annual transport cycle, this reduction can be attributed to the strong relaxation of the transport to a constant value. Additional factors affecting the amplitude of the model seasonal response are the coarse horizontal grid resolution and the related large lateral friction. On the basis of inverted echo sounder measurements in the region, *Garzoli and Garraffo* [1989] conclude that the principal motion of the confluence front is an east-west displacement of approximately 100 km, half the present model grid size, with an annual period related to variability in the latitude of maximum northward penetration of the Malvinas Current. Similarly, *Garzoli et al.* [1992] state that the amplitude of the meridional Brazil Current displacement during the year is roughly 2°, which the coarse model grid would barely resolve.

3.3. Influence of Variations in the Drake Passage Transport Forcing

The previous sections focused on experiments RBF (annual mean wind forcing) and RBFM (seasonal wind forcing), both of which used a fast Newtonian relaxation time resulting in a near-constant transport through Drake Passage, effectively 130 Sv. Longer relaxation times failed to bring the transport near to the desired value, the observed annual mean [*Whitworth et al.*, 1982]. In order to address the importance of Drake Passage transport fluctuations on the circulation in the Southwestern Atlantic, we present in this section the

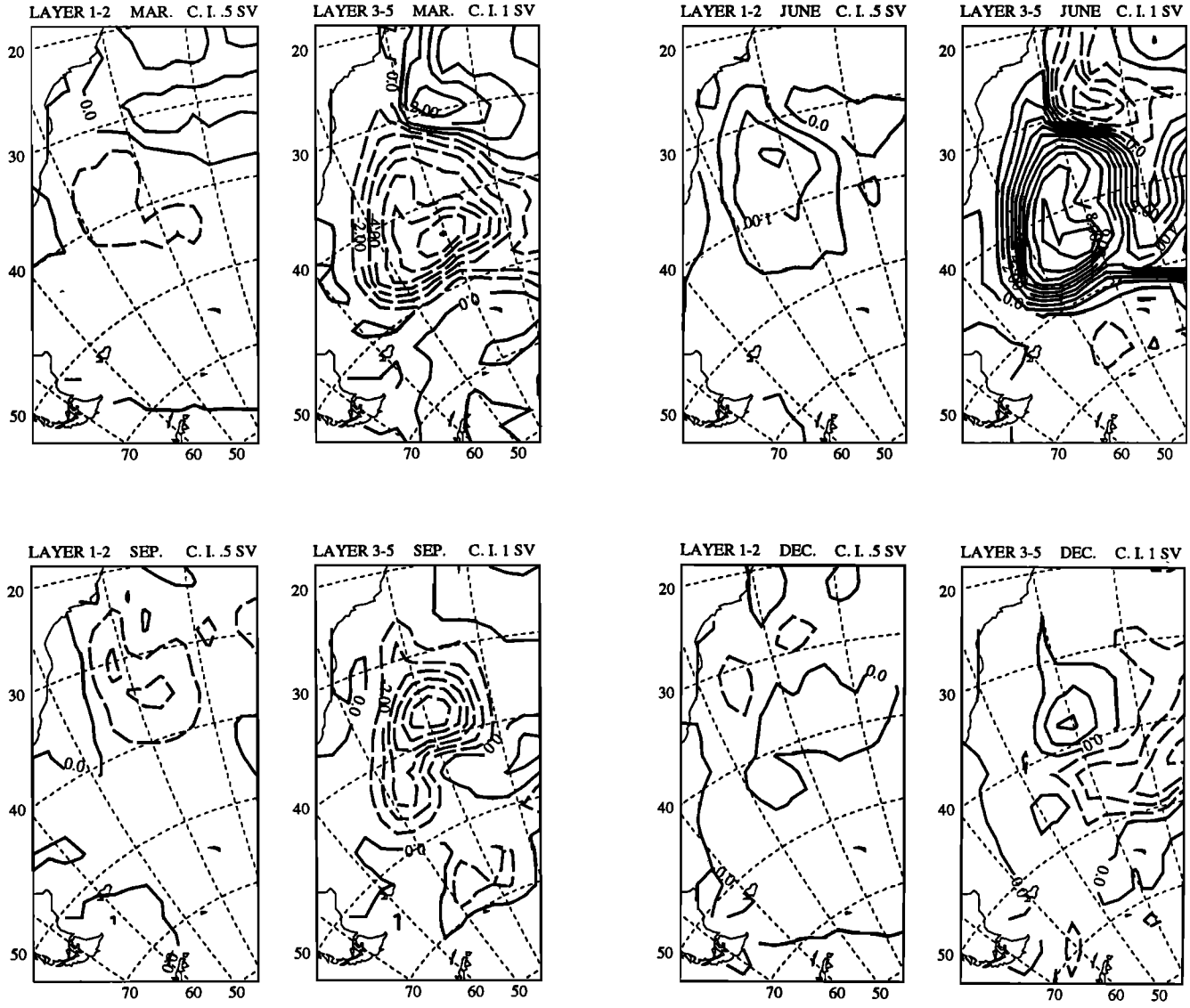

Figure 9. Mass flux streamfunction anomaly (relative to annual mean) for layers 1 and 2, and for layers 3, 4 and 5, for months of March, June, September, and December from average annual cycle of experiment RBFM.

results of experiments in which the transport is relaxed to values interpolated at each model time step from a 1-year series of daily transport values presented by *Whitworth* [1983], to which a 30-day low-pass filter has been applied (Figure 10a). The fluctuations in transport at Drake Passage are representative of wind forcing not only from the South Atlantic but also from the Indian and Pacific oceans. These experiments are forced by the HR83 climatological winds that were applied to experiments RBF and RBFM.

Two 5-year model integrations similar to case RBF (forcing by the HR83 annual mean winds) and case RBFM (forcing by the HR83 monthly winds), but allowing the forced Drake Passage transport value to vary at each time step according to the values of *Whitworth* [1983], produced annual cycles of transport at that location which essentially duplicated the input set of forcing values (Figure 10a). In the case of seasonal wind forcing, additional weak transport fluctuations were seen in the annual cycle as a direct response to the variations in the wind (not illustrated). However, at Drake Passage the relaxation mechanism remains the controlling factor in setting the model transport, as opposed to the wind forcing.

In the Malvinas transport, however, we expect to observe the influence both of variations in the local wind and of variations in the magnitude of the Drake Passage transport. In the case of constant forcing of the transport through the passage and seasonal forcing by the winds, the Malvinas transport cycle (Figure 10b, repeated from Figure 7b) possesses a clear semiannual signal related to the signal present in the zonally averaged wind stress curl over the region (section 3.2). If we now force the model by constant (annual mean) winds and impose the above variable forcing on the Drake Passage transport, the annual cycle of Malvinas transport (Fig-

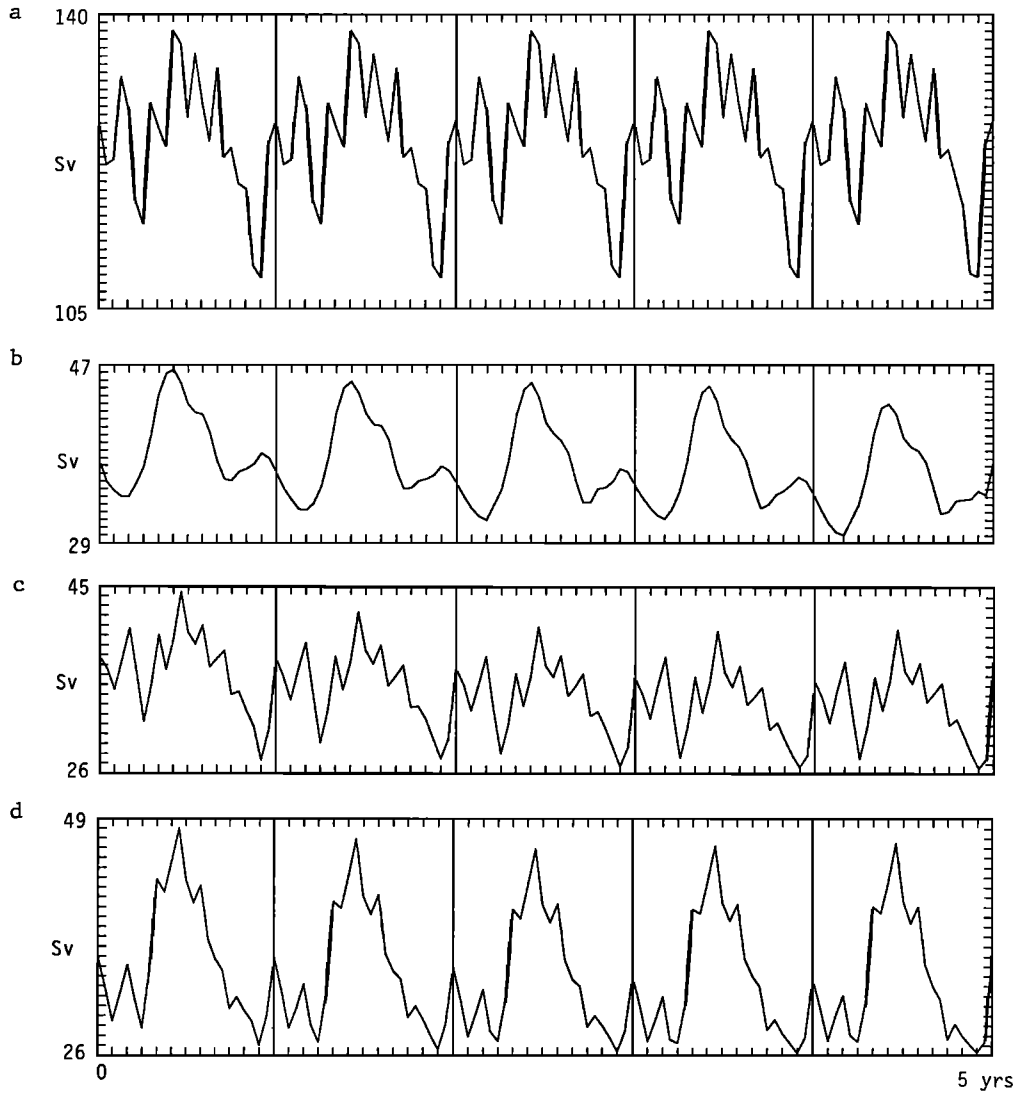

Figure 10. (a) 30-day low-pass filtered series of daily Drake Passage transport values from *Whitworth* [1983]. One-year record is repeated 5 times; (b) 5-year series of Malvinas Current transport across 45°S, experiment with constant Drake Passage transport forcing, monthly winds (repeated from Figure 7b); (c) 5-year series of Malvinas Current transport across 45°S, experiment with variable Drake Passage transport forcing, annual mean winds; (d) 5-year series of Malvinas Current transport across 45°S, experiment with variable Drake Passage transport forcing, monthly winds.

ure 10c) is nearly in phase with the Drake Passage forcing cycle (Figure 10a). The seasonal variations in ACC transport around the entire Southern Ocean, which are implicitly contained in the *Whitworth* [1983] Drake Passage transport values, are advected northward into the Malvinas Current.

If finally we allow both of the relevant model forcings to vary in time (the relaxation of Drake Passage transport and the forcing by the wind), the result in the Malvinas transport is the annual cycle displayed in Figure 10d. This cycle retains the semiannual character of the cycle shown in Figure 10b (a case in which only the wind forcing varied), with additional superimposed variations due to fluctuations in the Drake Passage transport forcing (Figure 10a).

4. Model Experiments Forced by Realistic Wind Data

The nature of the model forcing is relevant to the question of reduced amplitude of the model seasonal response, as discussed in section 3.2. *Smith et al.* [1990] found reduced amplitude in the model seasonal variations as compared to observations in their calculation for the North and Equatorial Atlantic, which was also forced by the HR83 monthly winds. In their analysis of the confluence region results from the *Semtner and Chervin* [1992] global model, *Garzoli et al.* [1992] also find that the spatial and temporal variability in the location of the modeled front is less than seen in the observations. They state that this can be attributed

in part to the lack of variability in the forcing by the HR83 climatological mean winds, which neglect the role of interannual wind stress variability in the determination of the seasonal response of the ocean [*Olson et al.*, 1988]. In this section, we address this issue by reporting on several experiments forced by realistic wind data for the years 1980-1989 from the European Center for Medium-range Weather Forecasting (ECMWF). In each of the model runs described in this section, the Drake Passage transport is relaxed to a constant value, as in experiments RBF and RBFM. There is no series of daily Drake Passage transport values available, such as the 1-year *Whitworth* [1983] time series, that corresponds to the 10-year time period of the ECMWF wind data. By holding constant the value to which we relax the Drake Passage transport, we forego a realistic amplitude for the annual cycle of transport at that location in the model (while achieving a realistic mean transport value). However, we are then able to concentrate on the influence of South Atlantic wind-forced variations in the Malvinas transport, the confluence location, and the Brazil Current transport.

4.1. Model Experiments Forced by Mean ECMWF Winds

In Figure 3b we show the mean stress vectors for the 1980-1989 wind data provided by the European Center for Medium-range Weather Forecasting (ECMWF), interpolated onto the rotated Mercator grid of Figure 1. In comparison to the climatology of HR83 (Figure 3a), the mean ECMWF winds are notably stronger in the region of westerlies extending from mid-basin to the Indian Ocean and particularly in the band of polar easterlies north of the Antarctic continent.

The model was integrated for 5 years with forcing by the mean ECMWF winds, beginning from the final year of case RBFM (section 3.2). We refer to this case as RBFE (Rough Bottom, Forced, mean ECMWF winds). All other parameters are identical to those of RBFM, and the model output was averaged over the final year of integration for display.

Figure 11 shows the layer 1 velocity vectors and barotropic streamfunction for case RBFE, for comparison to Figure 5 for case RBF. The ACC transport through Drake Passage remains at 128 Sv as in RBF. However, the maximum northward transport of the Malvinas Current, in the recirculation centered on ~ 45°S, reaches 85 Sv in RBFE, versus 68 Sv in RBF. In the subtropical gyre, the maximum southward Brazil Current transport increases only slightly, to 38 Sv in RBFE versus 35 Sv in RBF, and there is no discernible difference in the layer 1 velocity vectors or in the Brazil Current separation latitude (i.e., the locus of the layer outcrop) for the two cases.

4.2. Model Experiments Forced by 10-Year ECMWF Winds

Beginning from the final year of experiment RBFE, the model was integrated for 10 years with forcing by the full 10-year ECMWF wind data set. We refer to this experiment as RBFME (Rough Bottom, Forced, Monthly ECMWF winds). As an example of the variability that exists within the ECMWF data set, and consequently within the RBFME results, we show in Figure 12 the model-produced barotropic streamfunction for the months of April 1980 and September 1985. These two months represent extrema, over the 10-year model run, in transport both of the Brazil Current and of the ACC through Drake Passage. In the case of the Drake Passage transport, variations within the 10-year cycle represent a damped response to local variations in wind forcing, due to the strong relaxation of the mean transport to a constant value. The stress vectors for these two months (not illustrated) reveal that the late winter winds of September are notably stronger than the April winds in three regions: the southeast trades blowing toward the equator, the northerlies along the coast of Brazil, and the westerly winds through Drake Passage. In the April (autumn) winds, a more well-defined cyclonic stress pattern appears at the southern end of the basin, due to strengthening of the polar easterlies along the Antarctic coast.

The barotropic streamfunctions from the RBFME results at mid-April 1980 and mid-September 1985 (Figure 12) reflect the wind stress differences between those

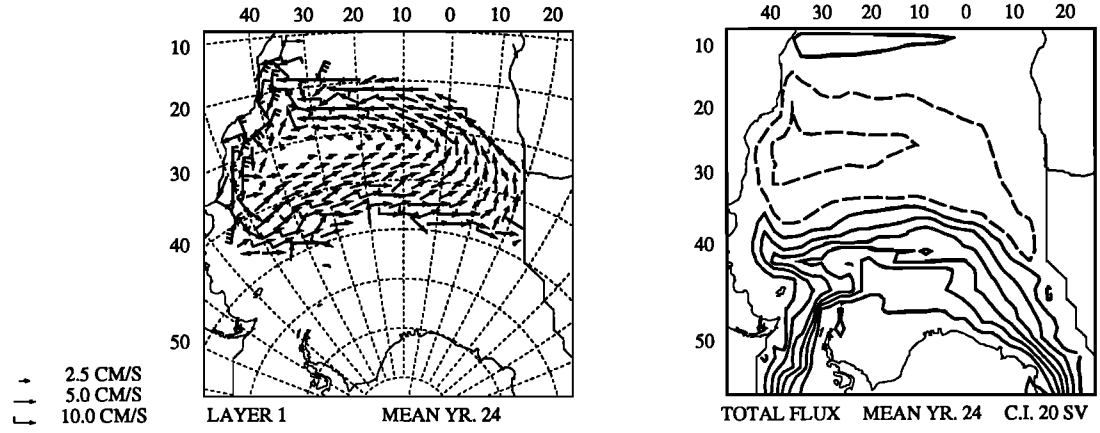

Figure 11. Layer 1 velocity vectors and barotropic mass flux streamfunction from experiment RBFE (rough bottom, forced, mean ECMWF winds).

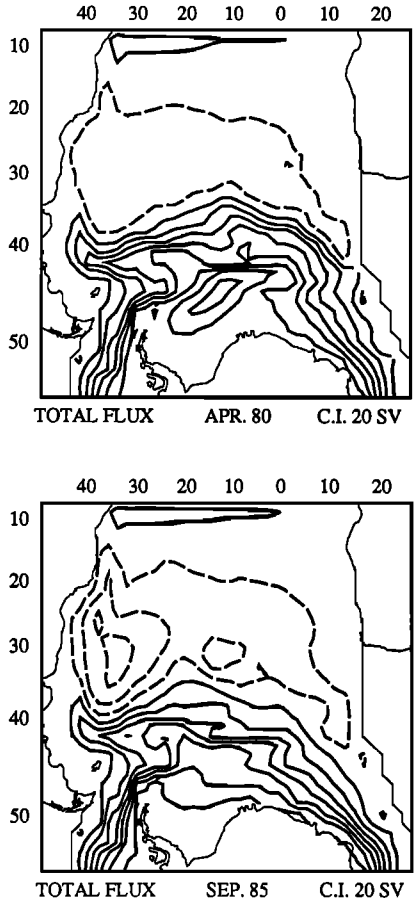

Figure 12. Barotropic mass flux streamfunction from experiment RBFME (rough bottom, forced, monthly ECMWF winds) for the months of April 1980 and September 1985.

two specific months. The transport in September 1985 is a maximum, over the entire 10-year RBFME run, both in the subtropical gyre (54 Sv Brazil Current transport across 30°S) and through Drake Passage (130 Sv). The opposite holds for the April 1980 results, which display the minimum transport both for the Brazil Current (28 Sv) and for Drake Passage (116 Sv). This correspondence, however, does not imply a direct (instantaneous) relation between stronger (or weaker) winds and greater (or lesser) transport in each of the principal currents which we are considering. In the case of the Malvinas Current, for example, the transport across 45°S is considerably higher in the April 1980 RBFME results (51 Sv) than in the results for September 1985 (32 Sv). This tendency for high (low) ACC transport to correlate with weaker (stronger) Malvinas flow appears to be reflected as well in the subpolar Weddell Gyre region. The cyclonic circulation of the Weddell sea is well developed in the April 1980 results, when the ACC is relatively weak and the Malvinas relatively strong, but is disrupted when the ACC transport is high, as in September 1985.

The offset in time between the annual cycle of transport through Drake Passage and the cycle of Malvinas transport across 45°S can easily be seen in the simpler RBFM results (Figure 7). In the case of RBFME, the 10-year model output allows us to construct time series of transport that are sufficiently long to assure statistical reliability [*Chelton*, 1982] in an analysis of the periodicity and interrelationships of the three principal South Atlantic currents, the Brazil, the Malvinas, and the ACC through Drake Passage. We have discussed earlier, in connection with RBFM, the existence of both annual and semiannual signals in the ACC transport and the relation of that cycle to the seasonal cycle of Malvinas transport. Here we examine the 240-point time series of transport through Drake Passage and of the Malvinas transport across 45°S from the RBFME results, stored every 15 days (Figures 13a and 13b respectively), and the variance-conserving energy spectrum of each series and squared coherence and phase relationship between the pair (Figure 13c). Each time series possesses a principal energy peak at the annual period and a secondary peak at the semiannual period, but the coherence between the series at the annual period falls below the 95% confidence limit. At the semiannual period, the series exhibit a high correlation, with a 180° phase shift existing between the pair as the Malvinas transport lags behind the Drake Passage transport. A 90-day shift in the start time of the Malvinas series produces a zero-degree phase lag between the two series at the semiannual period, although with coherence below the 95% confidence limit.

A similar analysis of the 10-year time series of Malvinas transport across 45°S together with the series of Brazil-Malvinas confluence latitude along 45°W shows that a peak in the energy spectrum of the confluence series, and a significant correlation between the two series, exists at the semiannual period only (Figure 14). (Recall that in section 3.2 we defined the "confluence" as the dividing line between the subtropical and subpolar gyres in the model results.) In contrast to the apparent 90-day offset between the Drake Passage and Malvinas series compared in Figure 13, here the phase lag between the Malvinas and confluence series at the semiannual period is near zero degrees.

Finally, we ask whether the phase relationships that exist in the model results among the 10-year cycles of Drake Passage transport, Malvinas transport across 45°S, and latitude of the confluence can be shown to extend to the Brazil Current region. Analysis of the time series of Drake Passage transport versus the series of Brazil Current transport across 30°S (not illustrated) reveals a distinct peak in the energy spectrum of the Brazil Current series at the annual period only, with a fragmented signal at higher frequencies. No significant coherence is seen between the two series at either the annual or semiannual periods. A similar result is obtained in comparing the Malvinas transport across 45°S to the Brazil Current series (Figure 15), although in this case the correlation between the two series lies marginally above the 95% confidence limit at the semiannual period. The high levels of coherence at the semiannual

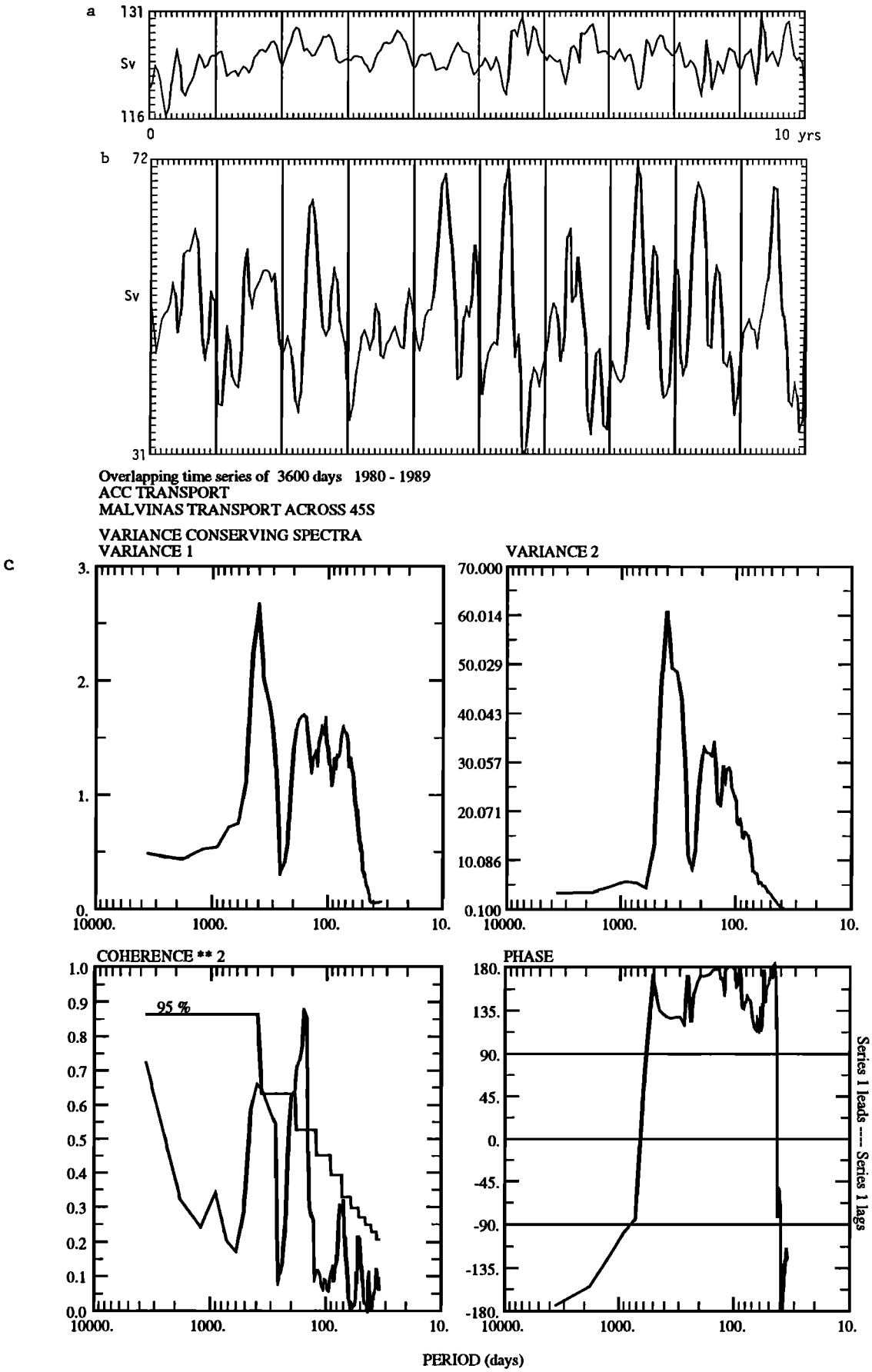

Figure 13. 10-year series from experiment RBFME of (a) Drake Passage transport and (b) Malvinas Current transport across 45°S. (c) Variance-conserving energy spectrum of each series and squared coherence and phase relationship between the pair.

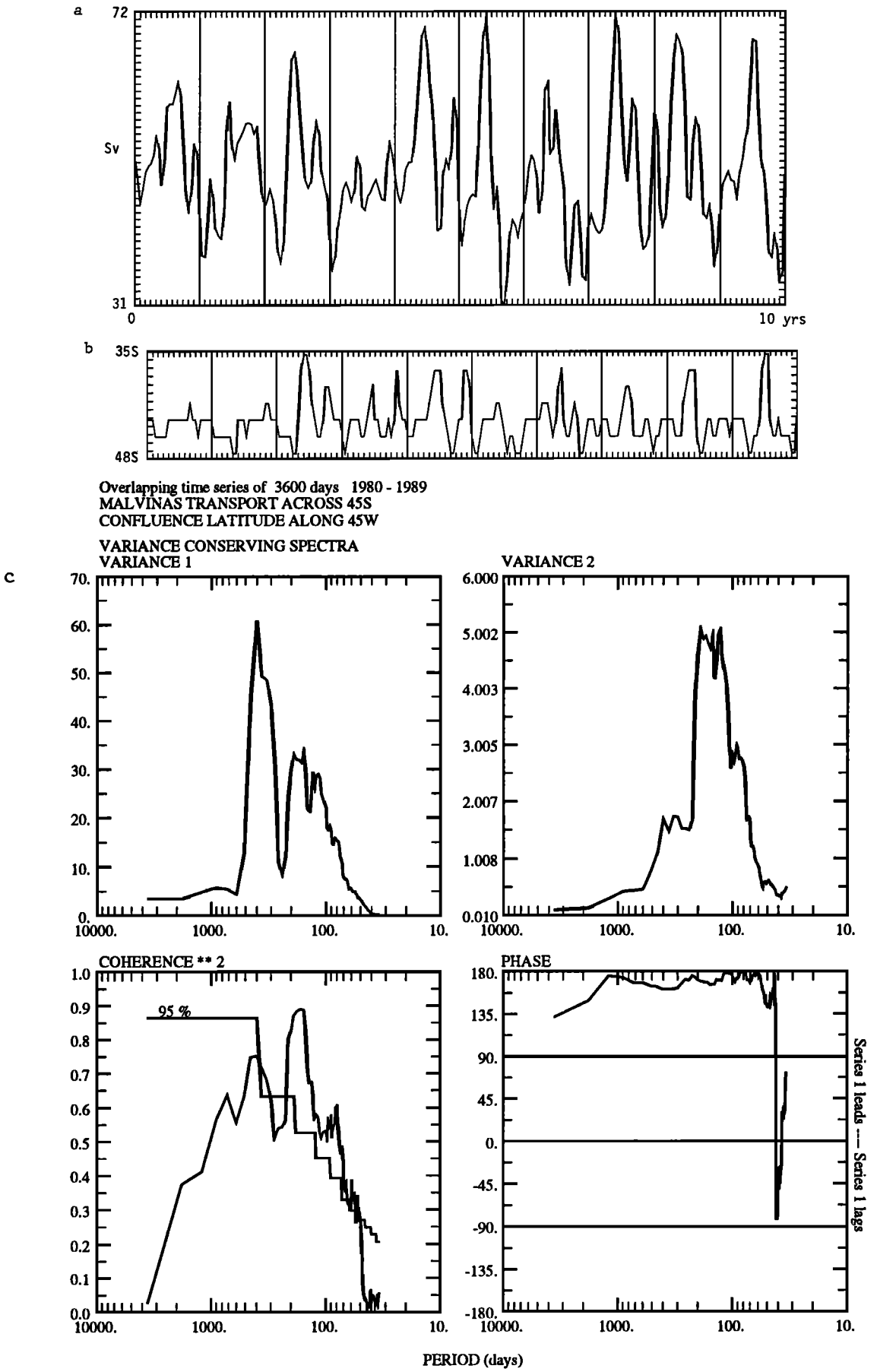

Figure 14. As in Fig. 13 but for (a) Malvinas Current transport across 45°S and (b) confluence latitude along 45°W.

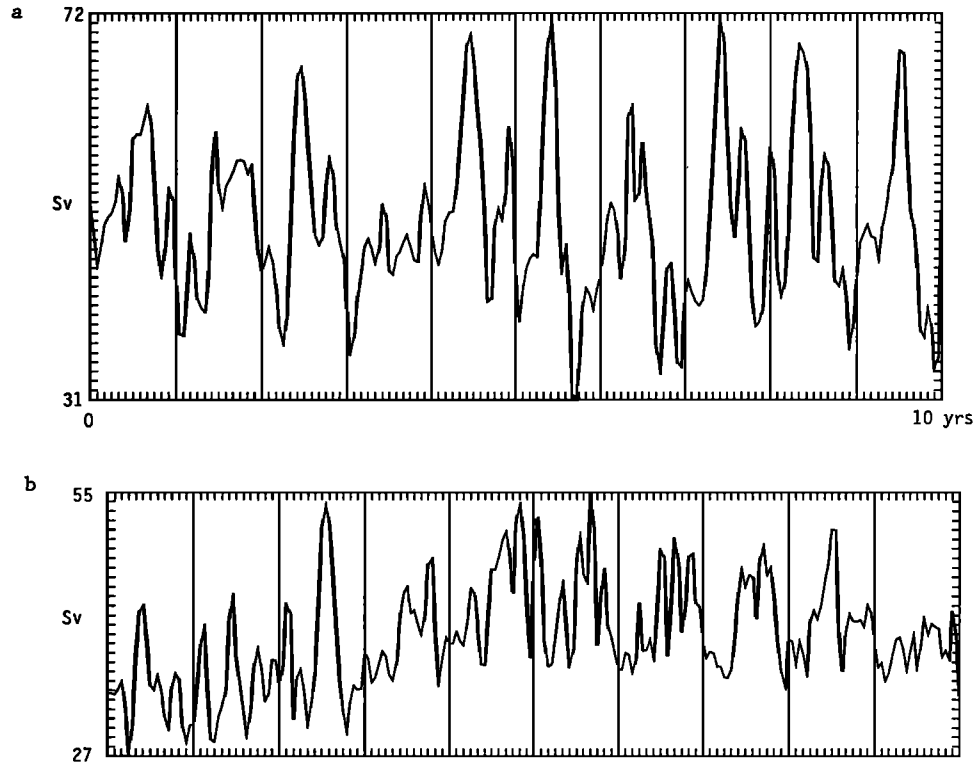

Figure 15. As in Fig. 13 but for (a) Malvinas Current transport across 45°S and (b) Brazil Current transport across 30°S.

period that were seen in Figures 13 and 14, relating to comparisons of the Drake Passage transport, Malvinas transport, and confluence latitude, are absent from these last two analyses.

5. Discussion

The results of our model runs forced by seasonally varying winds, both those obtained from climatology and those including interannual variations, are in agreement with recent studies indicating the presence of a significant semiannual signal in the variability of the South Atlantic circulation south of the Brazil-Malvinas confluence. In an analysis of the *Olson et al.* [1988] 3-year data set of SST in the confluence region, *Provost et al.* [1992] conclude that the ratio of the amplitude of the semiannual signal in SST to the annual amplitude increases from zero at 30°S to 45% at 50°S, with the semiannual frequency being associated with the semiannual wave present in the atmospheric forcing of the southern hemisphere [*Large and van Loon*, 1989]. *Garzoli and Giulivi* [1993], in an analysis based on a 15-month velocity record from inverted echo sounders in the confluence region [*Garzoli*, 1993], relate the annual cycles of north-south movement of the southern limit of the Brazil Current and the northern limit of the Malvinas Current to local changes in the curl of the wind stress, as calculated from the ECMWF wind data set for the time period of the observations. Since the curl of the HR83 climatological winds fails to account for the interannual variability found in the data, *Garzoli and Giulivi* [1993] conclude that the variability observed at the confluence has two principal components: local changes in the wind field south of the confluence, and seasonal variability of the wind stress curl integrated across the entire basin. The response due to the latter should consist of a barotropic component on the short term and an interannual baroclinic response. *Provost et al.* [1992] note also that the positions of the Brazil and Malvinas SST fronts exhibit significant interannual variations which, at certain locations, dominate the semiannual variations.

In addition to local changes in the curl of the wind stress, the correlation at the semiannual period between the ACC transport through Drake Passage and the Malvinas transport across 45°S could be attributable to remote effects such as the cyclonic (clockwise) passage of an edge wave around the basin, initiated by seasonal fluctuations in wind curl forcing in the Drake Passage-Malvinas region. The possible presence of such a mode in our coarse-resolution experiments was tested in a simplified two-layer model run, with an initial interface depth perturbation near the southwest corner of the basin and no external forcing at the surface. It was found that the propagation speed of the wave form around the edge of the basin was reduced by approximately 10% relative to the true wave speed, in agreement with the theoretical phase retardation due to the spatial differencing of the numerical grid [*Haltiner and Williams*, 1980].

c

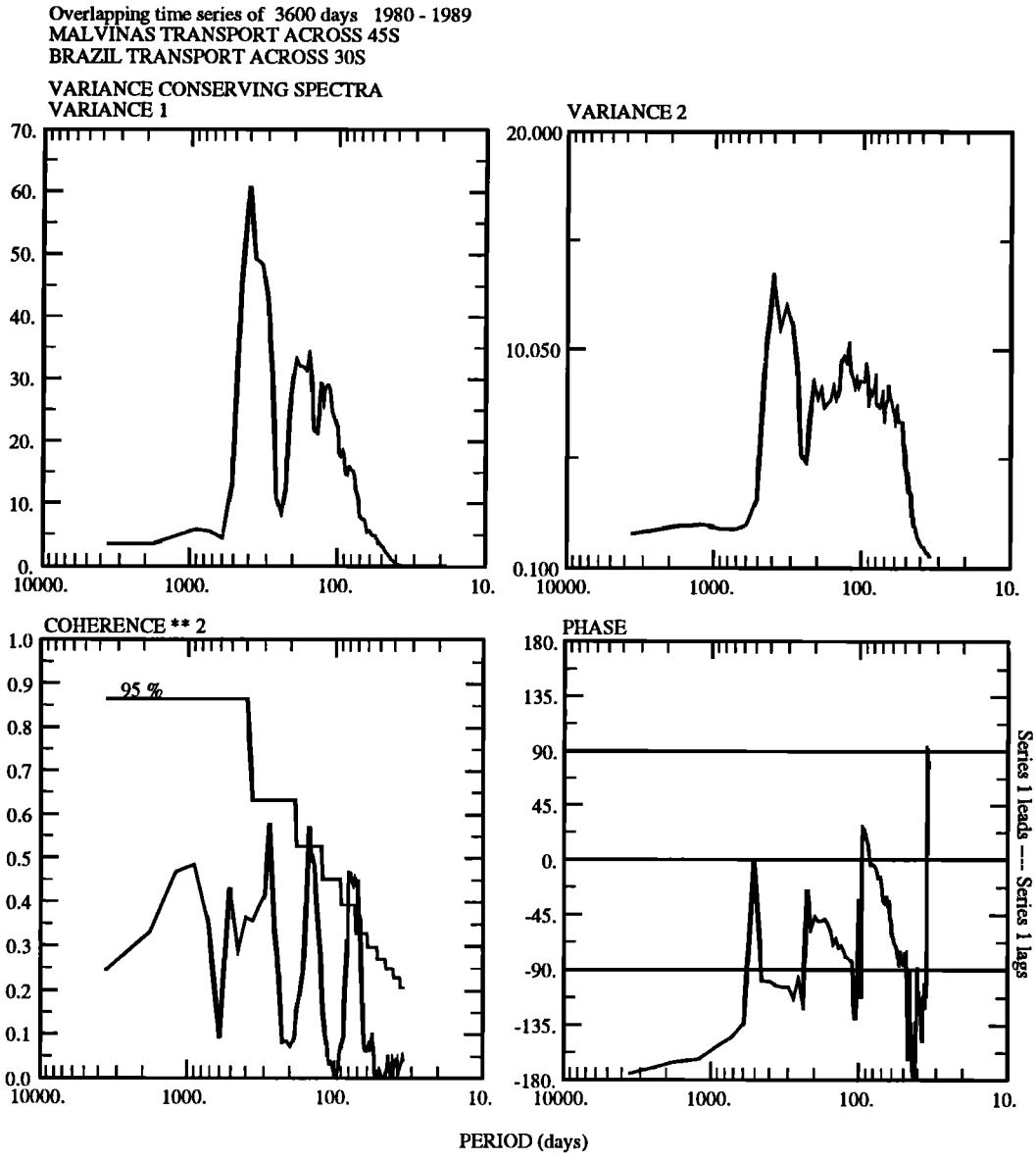

Figure 15. (continued)

This simplified experiment indicates that the large-scale semiannual signal forced by seasonal wind variations within the Drake Passage region can be carried northward by a Kelvin-type wave form into the region of the Brazil-Malvinas confluence, despite the coarse resolution of the model. As the wave form propagates along the coast, a number of factors may contribute to the decay of this signal, leaving the locally wind-forced annual oscillation as the predominant response in the model Brazil Current region. First, lateral friction must be mentioned as a straightforward cause of deterioration of the signal's strength. Second, the northward progression of the semiannual signal beyond the latitude of the Brazil-Malvinas confluence may be impeded by the southward flow of the Brazil Current itself. An experiment relevant to this issue was carried out by *Chassignet* [1988], in an eddy-resolving model of the South Atlantic and Indian oceans surrounding the southern part of Africa. *Chassignet* [1988] demonstrated the propagation of a Kelvin wave around the entire model basin, generated by a cyclonic ring off the tip of Africa. He found that the response to the edge mode was blocked in the region off the east coast of Africa, where the wave's northward passage was retarded by the southward movement of the Agulhas boundary current.

A third factor in decay of the northward propagation of a semiannual signal is related to the issue of momentum balance between currents flowing in opposite directions along a western boundary. Specifically, the largely barotropic edge wave, embedded in the northward flowing Malvinas, can lose energy as it attempts to cross the subtropical gyre outcrop line, along which the southward flowing Brazil travels. A 2 1/2 -layer f-plane

model experiment carried out by *Agra and Nof* [1993] considers the case of opposing currents of different densities, with the equatorward current (i.e., the Malvinas) being forced to dive underneath the less dense poleward flow (i.e., the Brazil) as both currents separate from the coast. The separation itself may be attributable in part to the momentum imparted on the poleward current by the opposing flow, even though the latter may be the weaker current of the two. In this scenario, which disregards the effects of wind forcing, the Malvinas can effectively push the Brazil Current to the north and offshore as it rides against the lower interface of the outcropping upper layer that represents the subtropical gyre. *Agra and Nof* [1993] propose this mechanism as one reason for the premature separation of the Brazil Current from the coast, which has been observed to occur at a latitude $\sim 10^{\circ}$ north of the climatological zero wind curl line [*Olson et al.*, 1988]. In an extension of this model study to a case including the effects of β, *Nof* [1993] further suggests that the observed seasonal oscillatory movement of the Brazil and Malvinas separation points [*Olson et al.*, 1988] may result from a β-induced southwestward migration, of rate on the order of the long Rossby wave speed, as well as from an imbalance in the alongshore drift induced by momentum as the two currents collide. The specific influence of the northward traveling edge wave on the change in momentum balance and on the separation point of the two currents should be explored further in the context of the *Agra and Nof* [1993] model.

6. Summary and Outlook

We have presented the results of a coarse-resolution, wind-driven isopycnic numerical model of the South Atlantic circulation, with emphasis on seasonal variations in the Brazil-Malvinas confluence region. Our initial experiments, using climatological wind forcing, demonstrated the effects of the inclusion of bottom topography (versus flat bottom integrations) in reducing the transport of the ACC through Drake Passage and in shifting the separation latitude of the Brazil Current to the north. The addition of seasonal climatological wind forcing allowed us to detect the presence of a semiannual signal in the annual transport cycles for both Drake Passage and the Malvinas Current, although the signal amplitude is limited in the former due to the relaxation of the transport to a constant value. When the value to which the Drake Passage transport is relaxed is allowed to vary in time, the semiannual wind-forced oscillation in the Malvinas region remains evident, with additional superimposed variations related to the variations in the transport forcing. In the Brazil Current transport cycle, the semiannual oscillation seen in the Malvinas was found to be significantly damped, and the calculated amplitude in each cycle was reduced relative to observations. A 10-year integration forced by the 1980-1989 ECMWF wind data set enabled the exploration of interannual variability in the South Atlantic circulation and provided more realistic forcing than the climatological winds, particularly in the region of the polar easterlies. The model output from this integration provided time series of sufficient length to permit analysis of the interrelationships of the major Southwestern Atlantic currents. While a high correlation at the semiannual period was found to exist among the cycles of Drake Passage transport, Malvinas Current transport, and seasonal movements of the Brazil-Malvinas confluence latitude, the Brazil Current transport cycle exhibited a significant energy peak only at the annual period. We conclude that the semiannual signal locally wind-forced south of the confluence is significantly damped before reaching the Brazil Current region by several factors: friction, the opposing flow of the current itself, and the inability of the denser Malvinas to penetrate the subtropical circulation that is confined to the upper model layers.

The model simulations have approached realism to an extent that allows a reasonable interpretation of the results regarding the wind-driven seasonal oscillations in the confluence region. We recognize that a realistic mean transport value through Drake Passage has been achieved by numerical means, a defect that might be overcome only by modeling the global circulation or at least the entire Southern Ocean. Here we look to attainable further refinements of the present model basin, specifically a reduction of the grid size and the inclusion of thermohaline forcing. A progression from the coarse horizontal grid of the present experiments to a finer mesh permitting the resolution of mesoscale eddies would allow a more detailed study of the role of edge modes in carrying a seasonal signal from the Drake Passage region into the Malvinas Current. An eddy-resolving model would also capture more realistic representations of the sharply sloping topography in the Drake Passage–Malvinas Plateau region and of the highly banded structure of the ACC velocity profile through Drake Passage [*Nowlin and Clifford*, 1982], as well as permit study of the eddy-filled region lying between the eastward extensions of the Brazil and Malvinas currents [*Olson et al.*, 1988]. Fine-resolution calculations are of principal importance to more detailed studies of seasonal variations in the confluence region, which as noted earlier may have a spatial range below the current model grid size [*Garzoli and Garraffo*, 1989; *Garzoli et al.*, 1992]. Decadal trends in the model output presented here, e.g., the increase in Brazil Current transport seen in Figure 15b, are as yet unconfirmed by observations and should be explored in longer-term fine-resolution integrations forced by observed interannual winds.

Looking beyond eddy-resolving wind-driven simulations, the addition of thermohaline forcing to the model will allow the study of processes linking North Atlantic deep water sources to the remainder of the world ocean

via the South Atlantic, thereby completing the global thermohaline circuit. Rings of the Agulhas Current, which may be modeled on an eddy-resolving grid, also play a role in the thermohaline circulation as they carry warm, salty Indian Ocean waters into the South Atlantic [*Olson and Evans*, 1986]. A recent South Atlantic model analysis by *Matano and Philander* [1993] estimates an equatorward heat flux of 0.19×10^{15} W across 30°S but does not consider seasonal variations in heat transport, which may be expected to occur in relation to the north-south movement of the Brazil Current extension [*Gordon*, 1981]. *Peterson and Stramma* [1991] point out that estimates of heat transport in the South Atlantic vary widely due to uncertainties both in computational methods and in the magnitude of seasonal and interannual variability south of 20°S. The incorporation of seasonal thermohaline forcing into the present South Atlantic model can be accomplished through the addition of a mixed layer above the isopycnic model interior, as *Bleck et al.* [1992] have recently demonstrated for the North Atlantic.

Appendix: Implementation of Cyclic Boundary Conditions

In order to model the flow of the ACC across the basin, cyclic lateral boundary conditions are imposed along the western and eastern ends of the channel extension at the southern end of the model ocean. The channel extension is discussed in section 2.2 and illustrated in Figure 1. For the purpose of describing the numerical implementation of the cyclic boundary conditions, we consider here a half-torus (Figure A1) as a simplified representation of the relevant part of the model domain. The cyclicity implies that the ends of the half-torus overlap, effectively creating the circular pathway that models the ACC.

The necessary extent of the overlap is determined by the horizontal staggering of the model variables, which in this case is the arrangement commonly referred to as the Arakawa C grid. Considering the grid stencils required to solve the finite difference equations in the model, it can be shown that no less than three rows of vorticity (Q in Figure A1) and zonal velocity (V) points, and two rows of mass (P) and meridional velocity (U) points, must overlap. The arrows drawn in Figure A1 indicate (for a sample cluster of grid points) the sense in which one cluster of variables is "copied" into another to create the overlap. The sense of the copy is such that variables nearest to the bottom of the half-torus (i.e., the boundary rows) receive their values from variables of the interior rows. Note that velocity points are copied with a change of sign. One central row of Q and V points is not copied; solutions of the momentum equations at the central V points, which should be identical on the two opposite sides except for a sign change, can be used to check for logical flaws in the copy process.

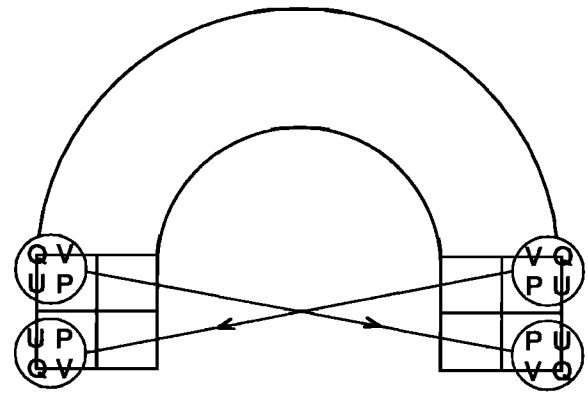

Figure A1. Schematic representation of implementation of cyclic boundary conditions.

Acknowledgments. Support for this work by the National Science Foundation under grants OCE-9102112 and OCE-9102560 is gratefully acknowledged. Computations were carried out at the National Center for Atmospheric Research, sponsored by the National Science Foundation. We thank Rainer Bleck for his contribution of the cyclic boundary condition logic and Claes G. H. Rooth for valuable comments on the manuscript.

References

Agra, C., and D. Nof, Collision and separation of boundary currents, *Deep-Sea Res.*,*40*, 2259–2282, 1993.

Anderson, D. L. T., and A. E. Gill, Spin-up of a stratified ocean, with applications to upwelling, *Deep-Sea Res.*, *22*, 583–596, 1975.

Anderson, D. L. T., K. Bryan, A. E. Gill, and R. C. Pacanowski, The transient response of the North Atlantic: Some model studies, *J. Geophys. Res.*, *84*, 4795–4815, 1979.

Bleck, R., and D. Boudra, Wind-driven spinup in eddy-resolving ocean models formulated in isopycnic and isobaric coordinates, *J. Geophys. Res.*, *91*, 7611–7621, 1986.

Bleck, R., and L. T. Smith, A wind-driven isopycnic coordinate model of the North and Equatorial Atlantic ocean, 1, Model development and supporting experiments, *J. Geophys. Res.*, *95*, 3273–3286, 1990.

Bleck, R., C. Rooth, D. Hu, and L. T. Smith, Salinity-driven transients in a wind- and thermohaline-forced isopycnic coordinate model of the North Atlantic, *J. Phys. Oceanogr.*, *22*, 1486–1505, 1992.

Bryan, K., and M. D. Cox, The circulation of the world ocean: A numerical study, I, A homogeneous model, *J. Phys. Oceanogr.*, *2*, 319–335, 1972.

Chassignet, E. P., Investigation of the dynamics of the Agulhas Current system in a numerical model, Ph.D. dissertation, 118 pp., University of Miami, Coral Gables, Fla., 1988.

Chassignet, E. P., and R. Bleck, Influence of outcropping on the separation of boundary currents, I, The wind-driven experiments, *J. Phys. Oceanogr.*, *23*, 1485–1507, 1993.

Chelton, D. B., Statistical reliability and the seasonal cycle: Comments on "Bottom pressure measurements across the

Antarctic Circumpolar Current and their relation to the wind", *Deep-Sea Res., 29*, 1381–1388, 1982.

Cox, M. D., A baroclinic numerical model of the world ocean: Preliminary results, in *Numerical Models of Ocean Circulation*, pp. 107–120, National Academy of Sciences, Washington, D. C., 1975.

Garzoli, S. L., Geostrophic velocity and transport variability in the Brazil-Malvinas confluence, *Deep-Sea Res.,40*, 1379–1403, 1993.

Garzoli, S. L., and Z. Garraffo, Transport, frontal motions and eddies at the Brazil-Malvinas confluence, *Deep-Sea Res., 36*, 681–703, 1989.

Garzoli, S. L., and C. Giulivi, What forces the variability of the South Western Atlantic boundary currents? *Deep-Sea Res.*, submitted, 1993.

Garzoli, S. L., Z. Garraffo, G. Podestá, and O. Brown, Analysis of a general circulation model product, 1, Frontal systems in the Brazil/Malvinas and Kuroshio/Oyashio regions, *J. Geophys. Res., 97*, 20117–20138, 1992.

Gordon, A. L., South Atlantic thermocline ventilation, *Deep-Sea Res., 28*, 1239–1264, 1981.

Gordon, A. L., Interocean exchange of thermocline water, *J. Geophys. Res., 91*, 5037–5046, 1986.

Gordon, A. L., Brazil-Malvinas confluence–1984, *Deep-Sea Res., 36*, 359–384, 1989.

Gordon, A. L., and C. L. Greengrove, Geostrophic circulation of the Brazil-Falkland confluence, *Deep-Sea Res., 33*, 573–585, 1986.

Haltiner, G. J., and R. T. Williams, *Numerical Prediction and Dynamic Meteorology*, 477 pp., John Wiley, New York, 1980.

Hellerman, S., and M. Rosenstein, Normal monthly wind stress over the world ocean with error estimates, *J. Phys. Oceanogr., 13*, 1093–1104, 1983.

Huang, R. X., Numerical simulation of wind-driven circulation in a subtropical/subpolar basin, *J. Phys. Oceanogr., 16*, 1636–1650, 1986.

Large, W. G., and H. van Loon, Large scale, low frequency variability of the 1979 FGGE surface buoy drifts and winds over the southern hemisphere, *J. Phys. Oceanogr., 19*, 216–232, 1989.

Levitus, S., Climatological Atlas of the World Ocean, *NOAA Prof. Pap. 13*, 173 pp., U.S. Dep. of Commer., Rockville, Md., 1982.

Matano, R. P., On the separation of the Brazil Current from the coast, *J. Phys. Oceanogr., 23*, 79–90, 1993.

Matano, R. P., and S. G. H. Philander, Heat and mass balances of the South Atlantic ocean calculated from a numerical model, *J. Geophys. Res., 98*, 977–984, 1993.

Matano, R. P., M. G. Schlax, and D. B. Chelton, Seasonal variability in the Southwestern Atlantic, *J. Geophys. Res., 98*, 18027–18035, 1993.

McWilliams, J. C., W. R. Holland, and J. H. S. Chow, A description of numerical Antarctic Circumpolar Currents, *Dyn. Atmos. Oceans, 2*, 213–291, 1978.

Nof, D., The β-induced drift of separated boundary currents, *Deep-Sea Res.,40*, 2243–2257, 1993.

Nowlin, W. D., Jr., and M. Clifford, The kinematic and thermohaline zonation of the Antarctic Circumpolar Current at Drake Passage, *J. Mar. Res., 40*, suppl., 481–507, 1982.

Oliger, J., and A. Sundström, Theoretical and practical aspects of some initial boundary value problems in fluid dynamics, *SIAM J. Appl. Math., 35*, 419–446, 1978.

Olson, D. B., and R. H. Evans, Rings of the Agulhas, *Deep-Sea Res., 33*, 27–42, 1986.

Olson, D. B., G. P. Podesta, R. H. Evans, and O. B. Brown, Temporal variations in the separation of Brazil and Malvinas currents, *Deep-Sea Res., 35*, 1971–1990, 1988.

Parsons, A. T., A two-layer model of Gulf Stream separation, *J. Fluid Mech., 39*, 511–528, 1969.

Peterson, R. G., On the transport of the Antarctic Circumpolar Current through Drake Passage and its relation to wind, *J. Geophys. Res., 93*, 13993–14004, 1988.

Peterson, R. G., The boundary currents in the western Argentine Basin, *Deep-Sea Res., 39*, 623–644, 1992.

Peterson, R. G., and L. Stramma, Upper-level circulation in the South Atlantic ocean, *Prog. Oceanogr., 26*, 1–73, 1991.

Provost, C., O. Garcia, and V. Garçon, Analysis of satellite sea surface temperature time series in the Brazil-Malvinas current confluence region: Dominance of the annual and semiannual periods, *J. Geophys. Res., 97*, 17841–17858, 1992.

Roemmich, D., The balance of geostrophic and Ekman transport in the tropical Atlantic Ocean, *J. Phys. Oceanogr., 13*, 1534–1539, 1983.

Semtner, A. J., Jr., and R. M. Chervin, A simulation of the global ocean circulation with resolved eddies, *J. Geophys. Res., 93*, 15502–15522, 1988.

Semtner, A. J., Jr., and R. M. Chervin, Ocean general circulation from a global eddy-resolving model, *J. Geophys. Res., 97*, 5493–5550, 1992.

Smagorinsky, J. S., General circulation experiments with the primitive equations, I, The basic experiment, *Mon. Weather Rev., 91*, 99–164, 1963.

Smith, L. T., Numerical simulations of stratified rotating flow over finite amplitude topography, *J. Phys. Oceanogr., 22*, 686–696, 1992.

Smith, L. T., D. B. Boudra, and R. Bleck, A wind-driven isopycnic coordinate model of the North and Equatorial Atlantic Ocean, 2, The Atlantic basin experiments, *J. Geophys. Res., 95*, 13105–13128, 1990.

Stommel, H. M., Asymmetry of interoceanic fresh-water and heat fluxes, *Proc. Natl. Acad. Sci. U.S.A., 77*, 2377–2381, 1980.

Stramma, L., Y. Ikeda, and R. G. Peterson, Geostrophic transport in the Brazil Current region north of 20°S, *Deep-Sea Res.,37*, 1875–1886, 1990.

Treguier, A. M., and J. C. McWilliams, Topographic influences on wind-driven, stratified flow in a β-plane channel: An idealized model for the Antarctic Circumpolar Current, *J. Phys. Oceanogr., 20*, 321–343, 1990.

Veronis, G., Model of world ocean circulation, I, Wind-driven, two-layer, *J. Mar. Res., 31*, 228–288, 1973.

Webb, D. J., P. D. Killworth, A. C. Coward, and S. R. Thompson, *The FRAM Atlas of the Southern Ocean*, National Environmental Research Council, Swindon, England, 1991.

Whitworth, T., III, Monitoring the transport of the Antarctic Circumpolar Current at Drake Passage, *J. Phys. Oceanogr., 13*, 2045–2057, 1983.

Whitworth, T., III, W. D. Nowlin, Jr., and S. J. Worley, The net transport of the Antarctic Circumpolar Current through Drake Passage, *J. Phys. Oceanogr., 12*, 960–971, 1982.

Wolff, J.-O., E. Maier-Reimer, and D. J. Olbers, Wind-

driven flow over topography in a zonal β-plane channel: A quasi-geostrophic model of the Antarctic Circumpolar Current, *J. Phys. Oceanogr.*, *21*, 236–264, 1991.

Zalesak, S. T., Fully multidimensional flux-corrected transport algorithms for fluids, *J. Comput. Phys.*, *31*, 335–362, 1979.

Zemba, J. C., The transport and structure of the Brazil Current between 27° and 36° South, Ph.D. dissertation, Mass. Inst. of Technol., Cambridge, 1991.

E. P. Chassignet, D. B. Olson, and L. T. Smith, Rosenstiel School of Marine and Atmospheric Science, University of Miami, 4600 Rickenbacker Cswy., Miami, FL 33149. (e-mail: echassignet@rsmas.miami.edu,dolson@rsmas.miami.edu, lsmith@rsmas.miami.edu)

(Received June 18, 1993; revised September 30, 1993; accepted November 17, 1993.)